Eur. J. Mineral.
2019, **31**, 755–774
Published online 6 June 2019



**To Christian Chopin, for 30 years of dedicated service to EJM**

# Lithium mineral evolution and ecology: comparison with boron and beryllium

Edward S. GREW[1,*], Grete HYSTAD[2], Myriam P. C. TOAPANTA[2], Ahmed ELEISH[3], Alexandra OSTROVERKHOVA[4], Joshua GOLDEN[5] and Robert M. HAZEN[6]

[1]School of Earth and Climate Sciences, 5790 Bryand Global Sciences Center, University of Maine, Orono, ME 04469-5790, USA
*Corresponding author, e-mail: esgrew@maine.edu
[2]Department of Mathematics, Statistics, and Computer Science, Purdue University Northwest, Hammond, IN 46323, USA
[3]Tetherless World Constellation, Rensselaer Polytechnic Institute, 110 8th Street, Troy, NY 12180, USA
[4]Department of Geology, Southern Illinois University, Parkinson, Mail Code 4324, Carbondale, IL 62901, USA
[5]Department of Geosciences, University of Arizona, Tucson, AZ 85721-0077, USA
[6]Geophysical Laboratory, Carnegie Institution for Science, 5251 Broad Branch Road NW, Washington, DC 20015, USA

**Abstract:** The idea that the mineralogical diversity now found at or near Earth's surface was not present for much of the Earth's history is the essence of mineral evolution, and the geological histories of the 118 Li, 120 Be, and 296 B minerals are not exceptions. Present crustal concentrations are generally too low for Li, Be, and B minerals to form (except tourmaline); this requires further enrichment by 1–2 orders of magnitude by processes such as partial melting and mobilization of fluids. As a result, minerals containing essential Li and Be are first reported in the geologic record at 3.0–3.1 Ga, later than Li-free tourmaline at 3.6 Ga. Spikes in species diversification coincides with increases in preserved juvenile crust and supercontinent assembly during the Precambrian Eon, followed by accelerated diversification during the Phanerozoic Eon. Mineral ecology concerns the present-day distribution, diversity, complexity, and abundance of minerals, including estimates of Earth's total mineral endowment, most recently by using large number of rare events (LNRE) models. Using Poisson-lognormal distribution and Bayesian methods, LNRE modeling yields an estimate of 1200–1500 total B mineral species, nearly triple the ~500 species estimate made in 2017, and from ~700 to ~800 total species for Li and Be. In considering how the total number of mineral species came to be present in Earth's crust, it is important to keep in mind the distinctions and the interplay between two very different histories: the geologic history of mineral formation, and the human history of mineral discovery. Mineral diversity has increased both with geologic time and with historic time, but only the latter strictly pertains to the accumulation curves that result from LNRE modeling. The Li minerals reported from the most localities would be expected to be discovered earliest in the historic search for new minerals and to have appeared earliest in Earth's history. However, data on Li minerals imply that factors other than number of present-day localities, at present totaling 3208 mineral/locality counts, play a major role in mineral ecology. More significant are the unique formation conditions at a handful of localities that produced a diverse suite of Li minerals rarely replicated elsewhere. The resulting present day non-random distribution of minerals contributes significantly to differences in the probabilities among species being discovered, which can have a profound impact on LNRE modeling.

**Key-words:** lithium; beryllium; boron; mineral evolution and ecology; new minerals; statistical mineralogy.

## 1. Introduction

The idea that the mineralogical diversity now found at or near Earth's surface was not present for much of Earth's history was first put forward by Zhabin (1979), who asked whether there could be an "evolution of mineral speciation on Earth," a question that has been the focus of Robert Hazen and his colleagues since 2008 (*e.g.*, Hazen *et al.*, 2008, 2012; Grew & Hazen, 2014). A related concept introduced by Hazen *et al.* (2015a) is mineral ecology, which in contrast to mineral evolution concerns the *present-day* processes (or processes at a given time in the past) influencing the distribution, diversity, complexity and abundance of minerals, including the interactions of minerals with abiotic and biotic systems in the environment. It is understood that the present-day situation is the result of all that has happened throughout Earth's history. The term "mineral ecology" had been used by Hommels *et al.* (1990) and Jones & Bennett (2017), but these authors were discussing microbial ecology where "mineral" refers to the geochemical environment of the microbes. Although the environment includes minerals, the authors' focus was on microbial diversity and

https://doi.org/10.1127/ejm/2019/0031-2862

distribution, not mineral species diversity and distribution. The term "mineral ecology" does not concern the impact of minerals on the environment. This concept would require a different term. Agusdinata *et al.* (2018) used the term "socio-ecology" in reference to impacts of lithium extraction, for example, the "socio-ecological consequences of mining activities and social justice issues on the local society" on page 8.

One aspect of mineral ecology is estimating the total number of mineral species present in Earth's crust today, that is, starting with the minerals already known and estimating the number yet to be discovered, Earth's so called "missing minerals." This endeavor has attracted the interest of mineralogists beginning over 80 years ago when Fersman (1938) estimated that the number of mineral species in Earth's crust probably would not exceed 3000 (Grew *et al.*, 2017a). However, a more quantitative mathematical approach to estimating the number of missing minerals only became available when Hystad *et al.* (2015a) showed that mineral species coupled with their localities conform to a Sichel's generalized inverse Gauss-Poisson (GIGP) large number of rare events (LNRE) distribution. Given the count in 2014 of 4831 species from 135 415 localities, *i.e.*, 652 856 mineral/locality pairs from the database at mindat.org, Hystad *et al.* (2015a) estimated a total of 6394 species, *i.e.*, about 1500 more species remained to be discovered assuming these "missing" minerals would be characterized using the same techniques. Hazen *et al.* (2015b) clearly realized that this is an underestimate because advances in technology have accelerated the rate of discovery and now 100–120 new mineral species are approved annually by the International Mineralogical Association Commission on New Minerals, Nomenclature and Classification (IMA CNMNC). In order to improve the estimate, Hystad *et al.* (2019) adopted a different approach, where the zero truncated Poisson-lognormal distribution is found to provide the best fit to the mineral frequency distribution using Bayesian methods. Employing this distribution, the total number of mineral species in Earth's crust was estimated to be 9308 with a 95% posterior interval estimated to be (8650; 10 070), *i.e.*, the estimated number of missing minerals is tripled. This total appears to be more reasonable when compared to the independent estimate of >15 300 minerals that could plausibly occur on terrestrial planets and moons throughout the cosmos (Hazen *et al.*, 2015a).

LNRE models have also been used to estimate the total number of missing mineral species for subsets of minerals, of which boron minerals have been studied in the greatest detail (Grew *et al.*, 2016, 2017a). In order to quantitatively evaluate estimates based on LNRE models, both the 295 B species discovered through 2017 and the 146 B minerals discovered through 1978 were modeled using a finite Zipf-Mandelbrot (fZM) distribution and a GIGP distribution. The 2017 dataset gave 50% higher totals than the 1978 dataset, *i.e.*, 459 ± 65.5 species (fZM) and 523 species (GIGP) *versus* 306 species (fZM) and 359 species (GIGP) for the 1978 dataset. This discrepancy was attributed largely to technological advances in analysis, most notably the electron microprobe, since the 1970s (Grew *et al.*, 2017a), one of the arguments made by Hystad *et al.* (2015b) to explain underestimates. Grew *et al.* (2017a) also expressed doubt that even the ~500 B species estimated from the 2017 dataset would be the "end of the story" because further technological advances as well as wider use of existing highly advanced technologies can be expected in the future.

The present paper applies the new approach (Hystad *et al.*, 2019) not only to B and Be minerals, previously modeled by Grew *et al.* (2016, 2017a and b) and Hystad *et al.* (2015b), but also to Li minerals, the mineral evolution and ecology of which have only been reported preliminarily in abstracts (*e.g.*, Grew *et al.*, 2018b). What these three elements have in common is the fragility of their nuclei, and consequently they are the least abundant elements lighter than Ca in the solar system, with CI chondrite abundances of 1.45, 0.0219, and 0.775 μg/g, respectively (Palme *et al.*, 2014). Despite their low abundance in Earth's upper continental crust, 21 μg/g Li, 2.1 μg/g Be, and 17 μg/g B (Rudnick & Gao, 2014), all three are quintessentially crustal elements.

In the present paper we review (1) the mineral evolution of Li minerals, that is, the history of their increasing diversity with the passage of geological time; (2) the mineral ecology of lithium minerals, in this case with a focus on the human history of their discovery and on estimates of Earth's total endowment at the present time; and (3) how these histories compare to those of B and Be minerals. A broader issue to be covered is how these two histories interact. Clearly the present distribution of Li minerals at or near Earth's surface, which is determined by geologic history, impacts the history of discovery by humans. Less obvious is whether the history of discovery and resulting LNRE distributions can inform us about the geologic history that resulted in the present distribution.

## 2. Definitions and criteria used in compiling the Li mineral database

### 2.1. Mineral species

We have chosen the Commission on New Minerals, Nomenclature and Classification of the International Mineralogical Association (CNMNC IMA) list as the basis for deciding what constitutes a mineral species primarily because this readily accessible list is widely recognized and accepted in the mineralogical community. Table S1 with bibliography Appendix S2 (freely available online as Supplementary Material linked to this article on the GeoScienceWorld website of the journal, https://pubs.geoscienceworld.org/eurjmin/) lists in alphabetical order the 118 minerals containing essential Li, including 114 of the 115 species approved by the CNMNC IMA together with their formulae and date of discovery, which were taken from the RRUFF website, http://rruff.info/ima/) on September 25, 2018.

The CNMNC list includes magnesiostaurolite and hectorite as Li minerals. Although Li is relatively abundant in both minerals, in neither mineral is Li the dominant constituent on the site occupied by Li, *i.e.*, Li is not an essential

constituent. On the basis of a crystal structure determination, Chopin *et al.* (2003) gave the ideal formula for the magnesiostaurolite end member as $^{A}\square_4{}^{B}Mg_4{}^{C}Al_{16}{}^{D}(Al_2\square_2)^{T}Si_8O_{40}{}^{X}[(OH)_2O_6]$ or simply $Mg_4Al_{18}Si_8O_{46}(OH)_2$, whereas the CNMNC list gives the formula as $Mg(Mg,Li)_3(Al,Mg)_{18}Si_8O_{44}(OH)_4$. As Chopin *et al.* (2003) did not formulate magnesiostaurolite as Li-bearing, we decided not to include it as a Li mineral. In contrast, Güven (1988) cited Li as a criterion to differentiate hectorite from other species of smectite. Although the CNMNC gives hectorite as a "questionable" species, clay mineralogists treat hectorite as a valid trioctahedral species in the smectite group (*e.g.*, Bailey, 1980; Guggenheim *et al.*, 2006; Clay Minerals Society, 2019), and consequently we have accepted hectorite as a valid Li mineral.

Following Grew *et al.* (2017a), we have included three tourmalines as potentially valid species, as well as the yet unnamed Zr analogue of baratovite as potentially valid. Group assignment is based largely on Back (2014) and Mills *et al.* (2009).

The date of discovery is the year when a full description of the species was published, or, at least, a partial description in an abstract. Publication of the mineral in the CNMNC Newsletters is not counted as the year of discovery unless this is the only information on a mineral, as is the case of some minerals discovered in the last year or so.

### 2.2. Localities

Grew *et al.* (2017a) noted that the definition of what constitutes a locality has turned out to be more difficult than what constitutes a species. Tables S1 and S2 with bibliography Appendix S1 gives the localities for Li minerals occurring at 15 localities or fewer; together with a few localities of more widespread minerals relevant to reported age of formation. Following Grew *et al.* (2016, 2017a), we adopted a more stringent definition of a locality than is used for the database at http://www.mindat.org. Examples of what mindat.org lists as multiple localities, but what we consider to be single localities are the pegmatites associated with Larvik plutonic complex in the Langesundsfjord area south of Oslo, Norway (Larsen, 2010) and with the Ilímaussaq complex in southwest Greenland. Each of these localities comprises several individual occurrences that we do not recognize as distinct localities because they are closely spaced and have identical ages. Reports of specimens from China and the former Soviet Union dating from the 1950s, 1960s, and early 1970s include only vague indications of localities (*e.g.*, "eastern Siberia", "Far East"), if any at all; in some cases, locality information can be obtained from later publications (*e.g.*, Pekov, 1998). Another difficulty is verification, particularly for minerals such as micas and amphiboles having a complex chemical compositions for which proper identification requires careful analysis, and many reports had to be rejected due to inadequate analyses. Other reports were rejected as the reported amount of Li was insufficient for the mineral to qualify as the Li-bearing species. The rejected reports are included in Table S2, but not in the locality counts. Because applying the above standards required consultation of the primary literature, it was practical only for Li minerals found at no more than about 15 localities worldwide, locality counts for minerals occurring at over 15 localities (except bityite) were taken from http://www.mindat.org (compilation for May 30, 2017). Counts based on occurrences > 15 localities could be approximations, but we have no way of knowing at what number of localities the approximations could be posing a problem. Because the Bayesian technique that we are currently using includes the entire frequency spectrum in the model, the number of localities for the more common minerals will introduce inaccuracies present in the mineral/locality counts taken from http://www.mindat.org.

### 2.3. Age of formation of Li minerals

As in the case of Be and B minerals, dating the formation of Li minerals can be problematic, because none of the Li minerals can be dated directly, and thus the ages of Li minerals listed in Tables S1–S3 have been inferred from ages obtained on associated minerals. For example, 31% of the oldest occurrences are pegmatites that have been dated by U–Pb isotopes on associated minerals in the pegmatite; this represents half of the Li minerals occurring in pegmatites, and thus in principle there is potential for more precise dating of Li minerals. Alternatively, Li minerals were dated on the basis of related geologic information, such as an age for the deposit in which these minerals are found. We have been mindful in considering whether Li minerals are younger than the dated mineral or deposit, and fortunately cases where Li minerals are significantly younger are fewer than in the case of B minerals. We were unable to find reliable ages for lithiophorite and swinefordite, as both minerals are supergene and considerably younger than the rocks with which they are associated. We did not attempt to get a maximum age for hectorite. Confirmed hectorite is found largely in Tertiary deposits (Table S2 and http://www.mindat.org), and appears to be supergene where it occurs in pre-Tertiary pegmatites.

### 2.4. Synthetic analogues of Li minerals

In order to evaluate the possibility that synthetic compounds are a source of potential new Li minerals, we reviewed the literature on syntheses involving Li. Following Grew *et al.* (2017a), we recognized synthetic compounds as analogues of minerals if they have the same composition and crystal structure as the mineral (Table S4 with bibliography Appendix S2), but in contrast to B minerals, we encountered few difficulties in identifying these analogues.

## 3. Evolution of lithium minerals

The geological history of lithium minerals reveals that this subset of the mineral kingdom has evolved in the sense that lithium minerals found today were not necessarily present in the past. Present crustal concentrations are generally too low for Li minerals, as well as Be and nearly all B minerals, to

form; their formation requires further enrichment by one to two orders of magnitude by processes such as partial melting and mobilization of fluids, which are associated with growth of continental crust. As a result, minerals containing essential Li and Be are first reported relatively late in the geologic record at 3.0–3.1 Ga (Grew & Hazen, 2014, and see below), *i.e.*, later than the oldest reported B minerals, which are Li-free tourmalines formed by metamorphism at 3.6 Ga of 3.7–3.8 Ga supracrustal rocks in the Isua belt, southwestern Greenland (Grew *et al.*, 2015).

Increases of mineral diversity with the passage of time can be expressed in two types of diagrams, which can be compared to curves for growth of continental crust (Fig. 1a). Cumulative diversity is based on the oldest reported occurrences in the geological record (Table S1). Reported ages are plotted cumulatively by adding each new mineral to the number of minerals already reported from older rocks (Fig. 1b). The second diagram (Fig. 1c) is a histogram giving an estimate of the number of Li minerals that formed in any one 50-Myr interval, which requires knowing the reported earliest, intermediate, and latest occurrences of each mineral in the geologic record (Tables S1–S3).

The oldest Li minerals so far reported in the geologic record are fluor-elbaite and polylithionite (as the dominant constituent of lepidolite) from granitic pegmatites associated with 3.0 Ga Sinceni pluton, Swaziland (Grew *et al.*, 2018a) and spodumene in granitic pegmatites of the lithium–cesium–tantalum (LCT) family from the 3.0 to 3.1 Ga New Consort mines, South Africa (Harris *et al.*, 1995). However, by the end of the Archean Eon, the number of Li minerals from LCT pegmatites or their aureoles (*e.g.*, holmquistite) reached 27, resulting in a spike of mineral diversity evident in the cumulative diagram (Fig. 1b) and in the histogram of estimates (Fig. 1c). This spike coincides not only with a spurt in the growth of preserved juvenile crust, but also with the assembly of the supercontinent Kenorland during the Late Archean (Kenoran) orogeny (Williams *et al.*, 1991; Hoffman, 1997). However, Bleeker (2003; see also Bleeker *et al.*, 2016) did not consider the existence of such a "sprawling" supercontinent as established, and favored instead a scenario involving the transient supercratons Vaalbara, Superia and Sclavia, which resulted from cratonization between ~3000 Ma and ~2500 Ma (Fig. 1b). Regardless of how the amalgamation prior to 2500 Ma is viewed, it was as effective in generating LCT pegmatites as was amalgamation of continental crust fragments to form supercontinents after 2000 Ma.

The increase in Li mineral diversity during the Proterozoic Eon was less marked than during Archean Eon. Compared to B (Grew *et al.*, 2016; Grew, 2017) and Be minerals (Grew & Hazen, 2014), the increases in Li mineral diversity corresponding to the assembly of Nuna and Rodinia and spurts in the growth of juvenile crust are modest. Environments in which Li minerals were found during the Proterozoic Eon broadened to include not only LCT granitic pegmatites (*e.g.*, Tip Top mine, South Dakota, USA), but also the Ivigtut cryolite deposit, Greenland; the peralkaline Igdlutalik dike, Greenland; and Mn deposits, *e.g.*, Kalahari, South Africa. Nonetheless, the number of Li minerals forming in any one 50-Myr interval increased only from 19 to 25 species, a proportional increase significantly less than those of either B or Be. In the Phanerozoic Eon, Li mineral diversity spikes dramatically, as is evident in both the cumulative diversity diagram and the histogram of estimated diversity. Preservation bias undoubtedly contributes to the diversity increase as the present-day exposure of continental crust younger than 1000 Ma also increases steeply (Fig. 1a). However, there are also substantial contributions to the Phanerozoic spike from rocks of unusual diversity, *e.g.*, peralkalic pegmatites at Dara-i-Pioz, Tazhikistan, and episyenites, which are non-magmatic hydrothermal rocks in the Eastern Pedriza Massif, Spain (Fig. 1c), as well as from the greater number of environments for Li minerals, including evaporites (*e.g.*, Penobsquis potash deposit, New Brunswick, Canada), skarns (*e.g.*, Xianghualing, Hunan Province, China), and the Vico volcanic complex (Table S2).

## 4. History of discovery of lithium minerals

Spodumene and petalite were first reported in 1800, the first Li minerals to be described. Subsequently, lithium was discovered in petalite (Arfwedson, 1818; Berzelius, 1818). Only 19 more Li minerals were discovered prior to 1945, but discoveries accelerated after 1945, and now approach three new minerals annually (Figs. 2 and 3a). Forty Li minerals (34%) have been synthesized (Table S4), but only 13 minerals (11%) were synthesized prior to discovery in nature. Proportions for Be are comparable with 32% of all Be minerals having been synthesized and 8% synthesized prior to discovery in nature (Grew, unpublished compilation), whereas for B the proportions are higher, 41% and 19%, respectively (Grew *et al.*, 2017a). These authors concluded that synthetic compounds have not been a promising source for predicting potential new B minerals, a conclusion even more apropos for Li and Be minerals.

Seventy five percent of Li minerals form solid solutions or are isostructural with other minerals, analogs not only to mica, amphibole, and tourmaline, but also to minerals in less widespread groups such as triphylite and milarite, whereas 25% have unique crystal structures. The surge of discoveries in the last 30 years is almost entirely due to finding such structural analogs (Fig. 3a), which has been abetted by revisions in nomenclature allowing for finer distinctions between species based on site occupancy, most notably in the tourmaline (Henry *et al.*, 2011) and amphibole (Hawthorne *et al.*, 2012) supergroups. In contrast, 59% of B minerals overall have unique crystal structures and despite the recent uptick in the number of isostructural species, *e.g.*, tourmalines, a significant proportion of new B minerals even now have unique structures (Fig. 3b). Be minerals also have larger proportion of unique structures, 48%, and thus, like B minerals, have greater inherent structural diversity than Li minerals.

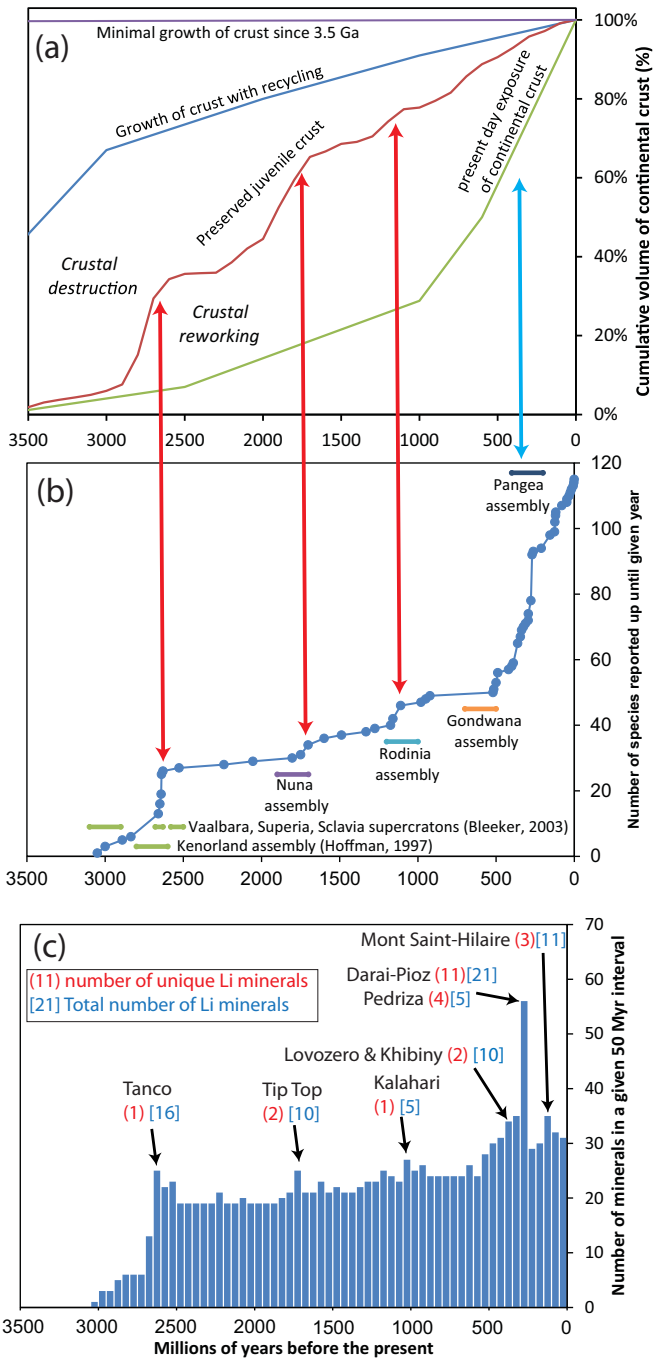


Fig. 1. Growth of continental crust *versus* Li mineral diversity. (a) Crustal growth, preserved juvenile crust and preserved continental crust plotted as a function of geologic time. Redrafted and modified from Grew (2017) and Hawkesworth *et al.* (2013). (b) Cumulative increase in the number of Li minerals as a function of geologic time based on the oldest reported occurrences in the geological record of 115 Li minerals (Table S1). The reported ages are plotted cumulatively by adding each new mineral to the number of minerals already reported from older rocks. Supercontinent names and ages of assembly are taken from Hoffman (1997) and supercraton names and ages taken from Bleeker (2003). Red arrows relate increases in cumulative diversity to growth of preserved juvenile continental crust, and blue arrow relates increase in cumulative diversity to present-day exposure of continental crust. (c) Histogram showing estimates of the number of Li minerals that had formed in a given 50 Myr interval based on the reported earliest, intermediate, and latest occurrences in the geologic record of 115 Li minerals (no age data is available on hectorite, lithiophorite, and swinefordite), together with reports from selected localities yielding a diverse suite of Li minerals (Tables S1–S3). The number of Li minerals found at a given locality and nowhere else is given in red font, whereas the total number of Li minerals found at a given locality is given in blue font. The full names of the localities and sources of data in addition to Tables S1–S3 are: Tanco mine, Manitoba, Canada (Selway *et al.*, 2000; Černý, 2005); Tip Top mine, South Dakota, USA (Campbell & Roberts, 1986; Loomis & Campbell, 2002); Kalahari manganese field, Northern Cape Province, South Africa; Lovozero and Khibiny alkaline complexes, Kola Peninsula, Russia (Pekov, 2000); Dara-i-Pioz glacier, Alai Range, Tajikistan; Eastern Pedriza Massif, Spanish Central System batholith, Spain; Mont Saint-Hilaire, Monteregian Hills, Quebec, Canada (Horváth & Gault, 1990).

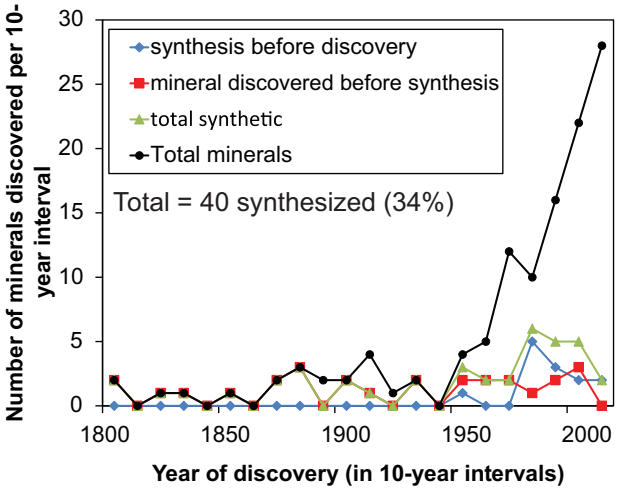


Fig. 2. History of discovery and synthesis of Li minerals expressed in terms of the number of minerals discovered or synthesized in 10-year intervals. Year of discovery taken from the RRUFF database. Information on syntheses taken from compilation in Table S4.

## 5. Large Number of Rare Event (LNRE) models of Li, Be, and B minerals

### 5.1. Background

LNRE models, used in calculating an author's vocabulary from word frequencies in the author's text (Baayen, 2001), can be applied to the count of mineral species so far discovered to calculate how many mineral species are ultimately present in Earth's crust today (*e.g.*, Hazen *et al.*, 2015a and b; Hystad *et al.*, 2015a and b). Mineral species diversity in this calculation is analogous to an author's vocabulary and mineral species/locality count with word count in a text, where total mineral species/locality counts are equal to the sum of minerals reported from one locality + twice the number of minerals reported from two localities + thrice the number of minerals reported from three localities, and so forth. However, in applying these models to minerals, Hazen, Hystad, and their co-authors cautioned that the assumptions in LNRE modeling include no changes in how minerals have been discovered during the more than two centuries since the beginning of mineral discoveries. Clearly there have been major changes over this period, and LNRE models encompass current and previous methods of discovery. For example, Grew *et al.* (2017a) explored the impact of one such change – advances in analytical technology – by (1) comparing the number of B minerals discovered through 2017 with the number of B minerals predicted for 2017 from the number of B minerals discovered up until 1978, when the electron microprobe displaced wet chemistry as the preferred method of chemical analysis, and (2) comparing the totals of B minerals predicted in 1978 with the totals predicted in 2017. In both cases the number of species for 2017 exceeded by 50% the predictions from the 1978 data set, *i.e.*, (1) 295 species discovered by 2017 *versus* 193 ± 7 species predicted from 1978 and (2) 459 ± 65.5 total

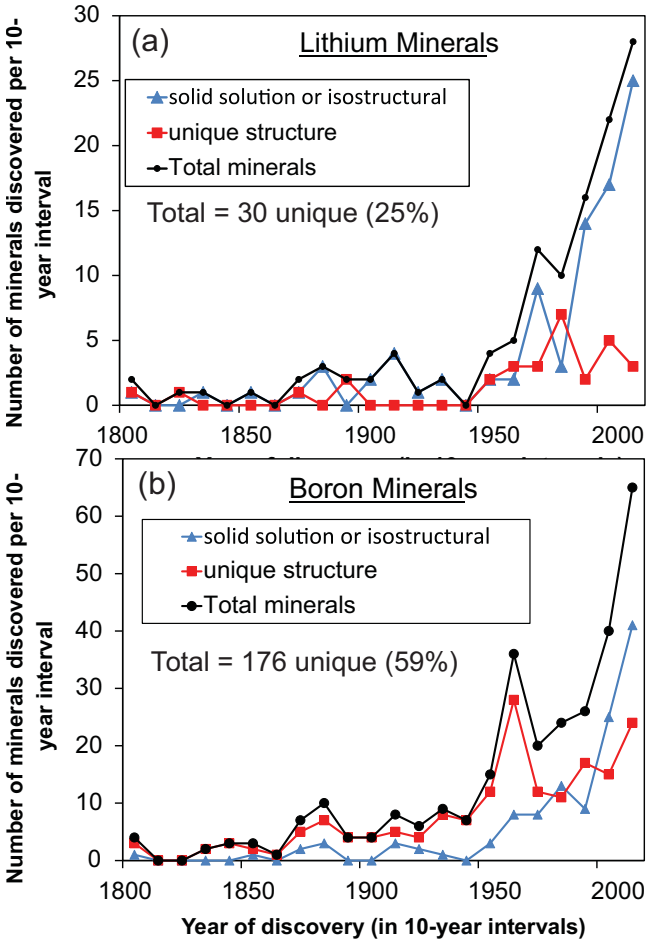


Fig. 3. History of discovery of Li and B minerals and relationships of Li and B minerals with each other and with other minerals. Year of discovery taken from the RRUFF database. (a) A Li mineral is considered unique if its structure is unlike that of any other mineral whether or not the mineral has been synthesized. In addition, one mineral in each group or series comprising only Li minerals is considered unique, *e.g.*, neptunite group, amblygonite-montebrasite, bertossite-palermoite, but not if the group includes minerals lacking Li, *e.g.*, triphylite, gainesite, tourmaline. Information on uniqueness taken from compilation in Table S4. (b) Boron minerals using the same criteria for defining uniqueness, and thus modified from Grew *et al.* (2017a, Fig. 5), which used different criteria for defining uniqueness.

species predicted from 2017 *versus* 306 total species predicted from 1978 using the fZM LNRE model (respectively 523 and 359 total species using GIGP model). However, the overall species predicted by LNRE models, 6394 species using the GIGP distribution, seems too low in view of the present rate of mineral discovery (>100 species a year, Hålenius *et al.*, 2018; Hazen *et al.*, 2018) and in comparison to other estimates, for example, the >15 300 plausible minerals that might occur collectively on all terrestrial bodies (Hazen *et al.*, 2015a). Hystad *et al.* (2019) have adopted the Bayesian approach to obtain the standard error directly from the simulations; in addition, a greater number of abundance distribution functions are available to examine than the previous technique used. The Poisson-lognormal distribution

is found to provide the best fit. Subsequently, the population size estimates obtained by Bayesian methods are compared to the empirical Bayes estimates. Population size is estimated as a function of sampling size from species accumulation curves. Using this approach, Hystad *et al.* (2019) estimated the total number of mineral species in Earth's crust to be 9308 and 95% posterior interval to be (8650, 10 070).

### 5.2. Methods

In view of the more plausible estimate for Earth's total mineral endowment reported by Hystad *et al.* (2019), we have applied their approach not only to lithium mineral occurrences reported through early 2018 (Tables S1 and S2), but also to the data on boron minerals, with a few minor modifications, *e.g.*, now 147 species through 1978 and 296 species through 2017, reported by Grew *et al.* (2017a), as well as to data on beryllium minerals, including data reported by Grew & Hazen (2014) and available at the database at mindat.org [note that Hystad *et al.* (2015b) relied entirely on mindat.org as a source of data]. In applying the approach of Hystad *et al.* (2019), we did the following: samples were simulated from the posterior distribution for the parameters by using the random walk Metropolis algorithm with the normal distribution used as the proposal distribution. For the different abundance distributions, different number of simulation runs were used. We refer the reader to Hystad *et al.* (2019), for the details. For the Poisson-lognormal distribution, we picked out every 500th iteration to reduce autocorrelation for beryllium and boron through 2017 and every 1000th iteration for boron through 1978. Nonetheless, we still have a high autocorrelation. For the GIGP distribution, we picked out every 60000th iteration to reduce autocorrelation.

Appendix S2 explains the method used in the simulation of lithium mineral ranking.

### 5.3. Results

Compared to the frequency spectra for all 4831 minerals recognized in 2014 (Hystad *et al.*, 2019), the agreement between the expected values of the frequency spectra calculated using the Poisson-lognormal distribution and observed frequency spectra is poor for B, and even worse for Li and Be (Fig. 4). The poor fits could be due to the small size of the sample as the fits become poorer with decreasing sample size. The poor fits imply that the predictive performance will also be poor.

Figure 5a shows the accumulation curve for Li minerals for the range of mineral/locality counts likely to be realized in the foreseeable future, whereas Fig. 5b shows the asymptotic approach to the mean at $10^7$ mineral/locality counts. Thus, to reach ~500 Li minerals would require sampling of $6 \times 10^6$ mineral/locality data, three orders of magnitude more than the 3208 localities sampled to date. Asymptotic approach to the mean also requires $10^7$ mineral/locality counts for Be and B.

The Poisson-lognormal distribution gives more than twice the total populations compared to GIGP total populations for B minerals. The GIGP calculations did not converge, casting doubt on their accuracy (Table 1), and thus have not been plotted in Fig. 6. The Poisson-lognormal median total population estimated for the B data obtained through 2017 is nearly double the median for the B data obtained through 1978, more than the 50% increase in estimates of total population reported by Grew *et al.* (2017a), who argued that access to smaller grains afforded by advanced analytical technology could explain the increase between 1978 and 2017. Since further technological advances are likely, the total population estimated using the method in Hystad *et al.* (2019) from the 2017 data is also likely to be an underestimate, and thus the upper range of the 95% posterior interval, *i.e.*, 1200–1500 B species, might be the better estimate for the total population of B minerals. By analogy, the total populations of Be and Li minerals could be in the upper range of their 95% posterior intervals, *i.e.*, ~700 to ~800 species. However, even with the ever accelerating rate of mineral discovery (*e.g.*, Figs. 2 and 3), it still may not be possible to discover these total populations anytime soon, given the large number of mineral/locality counts needed to reach them (Fig. 5).

### 5.4. Discussion

In considering questions about the total number of mineral species on Earth, we need to refine our understanding of the interplay between two very different histories: the geologic history of the formation of Li minerals, as examined by methods of mineral evolution such as the cumulative diversity diagram and histogram in Fig. 1b and c, and the human history of Li mineral discovery, as examined by the methods of mineral ecology such as LNRE modeling. There is no question that the present distribution of Li minerals at or near Earth's surface, which is determined by geologic history, impacts the human history of discovery. However, it remains an open question whether the history of discovery and resulting LNRE distributions can inform us about the geologic history and mineral evolution that produced the present distribution.

Hazen *et al.* (2015a) suggested that LNRE modeling can inform us regarding what minerals to expect if we were to play "the tape of Earth's history over again," analogous to "replaying the tape" of biological evolution, a thought experiment originally proposed by Gould (1989) and now being experimentally tested by biologists (Blount *et al.*, 2018). More specifically, they argued that the stochastic processes, which play a significant role in the diversity of less common minerals, can be modeled and that it is probable that, after 4.5 billion years of mineral evolution on an identical Earth-like planet, many of those minerals would differ from species known today even though deterministic factors would control the distribution of the most common minerals (see also Hystad *et al.*, 2015a and b). In other words, they suggested that LNRE models can inform us both about the history of discovery (human factors) and Earth's geological history.

In order to evaluate their argument that LNRE models can inform us about the human history of discovery and Earth's

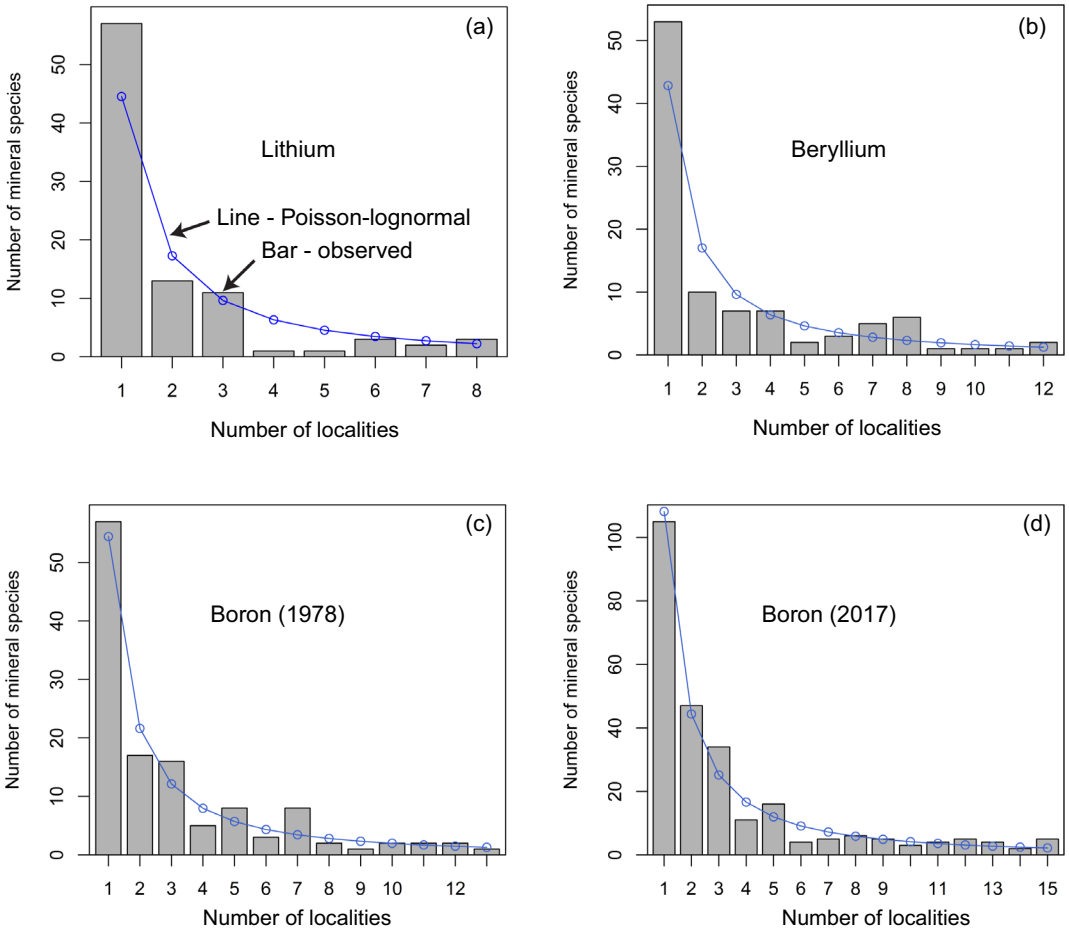


Fig. 4. Poisson-lognormal (line) and observed (bar) frequency spectra for 118 Li minerals (a), for 120 beryllium minerals (b), 147 boron minerals recognized in 1978 (c) and 296 boron minerals recognized in 2017 (d).

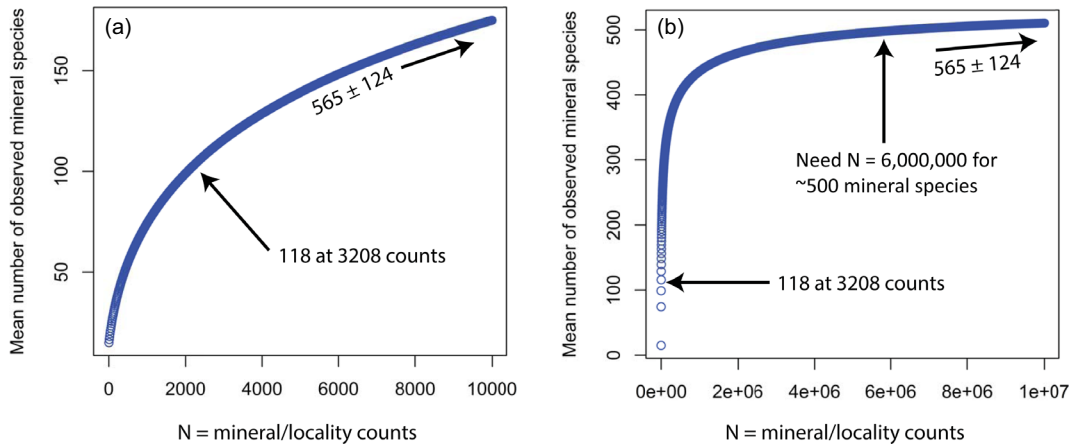


Fig. 5. Accumulation curves using the Poisson-lognormal model for lithium minerals for $N$ = 0–10 000 (a) and $N$ = 0–10 000 000 (b). The mineral/locality counts totaled 3208 in early 2018 (Table S1). The mean for the total population, $S$, is 565 with standard error of the mean of 15 and standard deviation of 124 (Table 1).

geological history, we can first reexamine the diagrams developed to illustrate geologic and human history, namely the cumulative diversity diagram in Fig. 1b, the history of discovery diagrams in Figs. 2 and 3, and the accumulation curve in Fig. 5, which results from LNRE modeling of lithium mineral discoveries. Comparisons with application

Table 1. Results of large-number of rare-event modeling of lithium, beryllium and boron minerals.

| Population | Distribution | Median | Mean | SE | SD | 95% Posterior interval | DIC | Accept rate | No. runs |
|---|---|---|---|---|---|---|---|---|---|
| All minerals up to 2014 (4831 species)* | Poisson-lognormal | 9308 | 9322 | 8 | 363 | (8650, 10 070) | 2875.70 | 45% | $10^6$ |
| Lithium (118 species) | Poisson-lognormal | 548 | 565 | 15 | 124 | (364, 861) | 232.6 | 45% | $10^6$ |
| Beryllium (120 species) | Poisson-lognormal | 511 | 519 | 3.8 | 115.1 | (322, 772) | 235.8 | 42% | $10^6$ |
| Boron up to 1978 (147 species) | Poisson-lognormal | 572 | 578 | 18.3 | 134.2 | (345, 868) | 206.3 | 37.8% | $2 \times 10^6$ |
| Boron up to 2017 (296 species) | Poisson-lognormal | 1020 | 1043 | 33.8 | 212 .1 | (690, 1527) | 303.1 | 39% | $10^6$ |
| Lithium (118 species) | GIGP | did not converge | – | – | – | – | – | 66% | $2 \times 10^7$ |
| Beryllium (120 species) | GIGP | did not converge | – | – | – | – | – | 55% | $10^7$ |
| Boron up to 1978 (147 species) | GIGP | 259, did not quite converge | 280 | 3.8 | 85.3242 | (205, 520) | 221.7 | 41% | $2 \times 10^7$ |
| Boron up to 2017 (296 species) | GIGP | 483 did not quite converge | 493 | 2.6 | 58.9 | (409, 622) | 628.3 | 45% | $2 \times 10^7$ |

*Notes*: The median, mean, standard error of the mean (SE), empirical standard deviation (SD), 95% posterior intervals, and the deviance information criterion (DIC) for the population size $S$ using Bayesian methods. Acceptance rate is the fraction of the simulations in the Metropolis algorithm that is accepted. GIGP – generalized inverse Gauss-Poisson. *Data from Hystad *et al.* (2019).

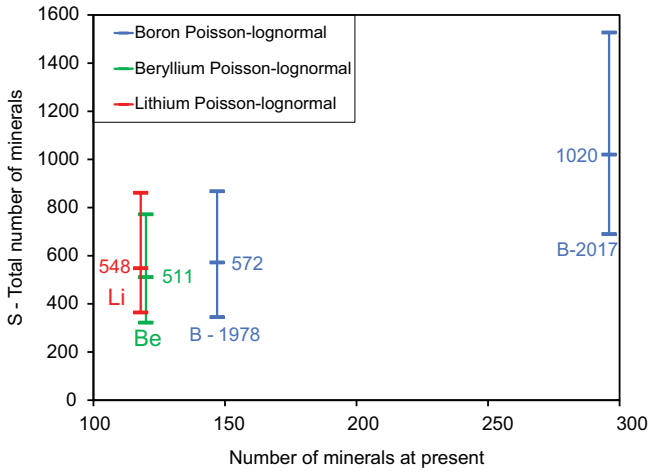


Fig. 6. Median values for $S$ (colored numbers) and 95% posterior intervals for Li, Be, and B minerals, last for species discovered by 1978 and by 2017, using the Poisson-lognormal model. Based on data in Table 1.

of LNRE models in linguistics (*e.g.*, Baayen, 2001; Piantadosi, 2014) can be instructive. The "total minerals" curve for Li minerals in Figs. 2 and 3a can be redrafted to give the cumulative discovery curve in Fig. 7a, which is generated by adding each newly discovered mineral to the number of minerals already discovered. The cumulative discovery curve differs from the cumulative diversity curve in that the **x**-axis is historic time instead of geologic time. We have also plotted a cumulative discovery curve for the subset of 14 Li minerals occurring in the Alai Range of Tajikistan and Kyrgyzstan (Fig. 7b) because we also have mineral/locality counts for these 14 minerals (Table 2). New mineral discoveries plotted as a function of mineral/locality counts gives us an accumulation curve (Fig. 7c) analogous to that shown in Fig. 5. Thus the accumulation curve is equivalent to the cumulative discovery curve. If we had the mineral locality counts for all Li minerals, we could plot an observed accumulation curve to compare with the modeled curve in Fig. 5. However, the relationship between the accumulation curve and cumulative diversity curve is much less obvious, since geologic age is not a factor in creating the accumulative curve. The latter considers mineral ecology, the number of minerals at one point in geologic time, namely the present, and assumes that the total number of minerals did not change and remains constant while species are being discovered through study of mineral localities. This approach is analogous to accumulating vocabulary as words are counted in stages in a literary work that is already written, *e.g.*, *Alice in Wonderland* (Baayen, 2001, p. 13).

An approach to relate accumulation and cumulative diversity curves such as Fig. 5a and 1b, respectively, is to compare the Zipf rank to the year of discovery (Fig. 7a) and to the age of earliest reported occurrence in the geologic record (Fig. 1b). Table 3 and Fig. 8 give (1) the Zipf rank, where the minerals occurring at the largest number of localities have the lowest rank (Baayen, 2001, p. 13), (2) a rank that increases with increasing discovery date of a mineral, and (3) a rank that increases with decreasing age of the reported first occurrence of a mineral in the geologic record. Only 37 Li minerals are listed as Zipf rank becomes more arbitrary at higher ranks, because ranks are arbitrarily assigned to minerals occurring at the same number of localities, which is more frequently the case for Li minerals occurring at three and fewer localities (Fig. 4a). In principle, we would expect that the most abundant minerals (lowest Zipf rank) not only to be discovered first, but also to appear more frequently in the geologic record, that is, over greater period of geological time, including the oldest rocks. Moreover, a simulation based on the mode of multiple runs shows that a nearly ideal 1:1 ratio could be expected for Zipf rank up to 40 (Fig. 9a). A prime example is spodumene, which is ranked first in all three rankings; other examples

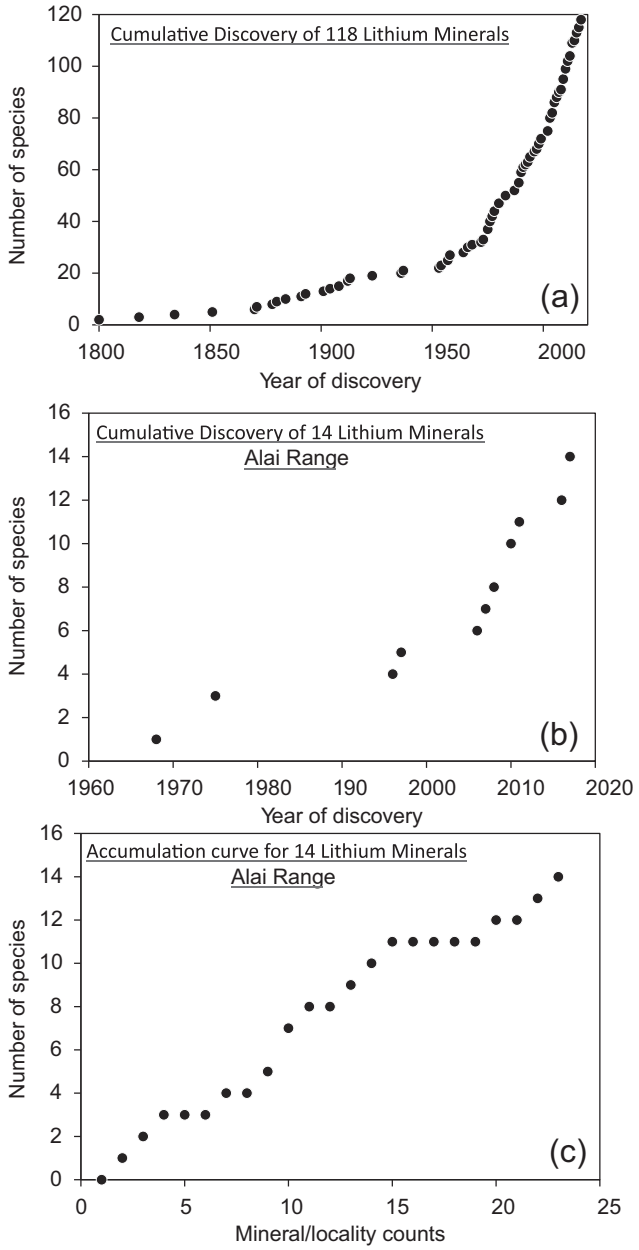


Fig. 7. (a) Cumulative increase in the number of Li minerals as a function of the year of discovery. The reported discovery years are plotted cumulatively by adding each new mineral to the number of minerals already discovered. Data are the same as used for total Li minerals in Figs. 2 and 3. (b) Cumulative increase of Li minerals in the Alai Range based on Table 2 constructed by the same procedure as in A. (c) Accumulation curve based on the data in Table 2, but in terms of mineral/locality counts instead of discovery date.

Table 2. Lithium minerals occurring in the Darai-Pioz and Hodzha-Achkan alkaline massifs, Alai Range, Tajikistan and Kyrgyzstan.

| Mineral | Date | Mineral/locality counts | New mineral |
|---|---|---|---|
| Neptunite | 1967 | 1 | 0 |
| **Sogdianite** | 1968 | 2 | 1 |
| **Baratovite** | 1975 | 3 | 2 |
| **Darapiosite** | 1975 | 4 | 3 |
| Polylithionite | 1975 | 5 | 3 |
| Zektzerite | 1992 | 6 | 3 |
| **Dusmatovite** | 1996 | 7 | 4 |
| Tainiolite | 1996 | 8 | 4 |
| **Berezanskite** | 1997 | 9 | 5 |
| **Sokolovaite** | 2006 | 10 | 7 |
| **Faizievite** | 2007 | 11 | 8 |
| **Nalivkinite** | 2008 | 12 | 8 |
| **Aleksandrovite** | 2010 | 13 | 9 |
| **Unnamed Zr analogue of baratovite** | 2010 | 14 | 10 |
| **Orlovite** | 2011 | 15 | 11 |
| Sugilite | 2011 | 16 | 11 |
| Katayamalite | 2013 | 17 | 11 |
| Baratovite (H.-A.) | 2013 | 18 | 11 |
| Katayamalite (H.-A.) | 2013 | 19 | 11 |
| **Bulgakite** | 2016 | 20 | 12 |
| Brannockite | 2016 | 21 | 12 |
| **Garmite** | 2017 | 22 | 13 |
| **Gorbunovite** | 2017 | 23 | 14 |

*Note*: Bold indicates mineral for which the Alai Range is the type locality. Date is the year mineral was reported or discovered in the Alai Range. All dates pertain to occurrence at Darai-Pioz except for second occurrences at Hodzha-Achkan indicated by H.-A. Sources of data are given in Table S1.

are amblygonite and montebrasite, which are uniformly ranked low. However, the linear fit to the discovery date data gives a coefficient of correlation ($R^2$) of less than 0.1, and thus the low positive slope may not be statistically significant (Fig. 8), implying factors other than number of present-day localities determine rank for the dates of discovery. Hystad *et al.* (2015b) reported an inverse relationship between the proportion of missing minerals on the one hand and bright colors, high luster, and tendency to form macroscopic euhedral crystals on the other. Their research also revealed that targeted searches and economic importance can lead to a lower proportion of missing minerals for some groups sorted by major-element chemistry. Similar human factors could also explain the poor correlation between discovery dates and Zipf rank in Fig. 8. Another contributing factor could be failure to distinguish different end members and delays in obtaining official approval of these end members, for example, elbaite is a conspicuous example with a discovery date rank of 105 due to its official approval as a species not being given until 2013.

The increase in rank by age of reported earliest appearance with Zipf rank gives a coefficient of correlation ($R^2$) of 0.49, and the linear fit has a clear positive slope near unity and passes close to the origin as would be expected in principle. Moreover, the simulation based on a single run gives a similar result for Zipf rank up to 40 – scatter about the ideal 1:1 line passing through the origin (Fig. 9b). Preservation bias undoubtedly contributes to the scatter in Fig. 8, especially for Archean occurrences, as Archean crust constitutes <10% of presently exposed continental crust (Fig. 1a). However, another factor could be that distinctive conditions developed at certain times in the geologic past that have not repeated since. The spikes in Li mineral diversity in Fig. 1c may reflect such special conditions, as the suite of

Table 3. The 37 most abundant Li minerals listed by their Zipf rank, with comparison to discovery date and earliest reported occurrence in the geologic record.

| Mineral name | Formula | Number of localities | Zipf rank | Order of increasing discovery date | Order of earliest occurrence |
|---|---|---|---|---|---|
| Spodumene | $LiAlSi_2O_6$ | 620 | 1 | 1 | 1 |
| Elbaite | $Na(Al_{1.5}Li_{1.5})Al_6(Si_6O_{18})(BO_3)_3(OH)_3OH$ | 506 | 2 | 105 | 14 |
| Triphylite | $LiFe^{2+}PO_4$ | 295 | 3 | 4 | 20 |
| Amblygonite | $LiAlPO_4F$ | 208 | 4 | 3 | 7 |
| Lithiophorite | $(Al,Li)Mn^{4+}O_2(OH)_2$ | 205 | 5 | 6 | – |
| Montebrasite | $LiAlPO_4(OH)$ | 185 | 6 | 7 | 8 |
| Cookeite | $(Al,Li)_3Al_2(Si,Al)_4O_{10}(OH)_8$ | 173 | 7 | 29 | 9 |
| Lithiophilite | $LiMn^{2+}PO_4$ | 137 | 8 | 8 | 4 |
| Petalite | $LiAlSi_4O_{10}$ | 111 | 9 | 2 | 17 |
| Polylithionite | $KLi_2AlSi_4O_{10}F_2$ | 86 | 10 | 10 | 2 |
| Ferrisicklerite | $Li_{1-x}(Fe^{3+},Mn^{2+})PO_4$ | 73 | 11 | 21 | 5 |
| Sicklerite | $Li_{1-x}(Mn^{2+},Fe^{3+})PO_4$ | 53 | 12 | 16 | 6 |
| Neptunite | $KNa_2LiFe^{2+}{}_2Ti_2Si_8O_{24}$ | 50 | 13 | 12 | 38 |
| Holmquistite | $\square Li_2(Mg_3Al_2)Si_8O_{22}(OH)_2$ | 37 | 14 | 18 | 10 |
| Tainiolite | $KLiMg_2Si_4O_{10}F_2$ | 37 | 15 | 13 | 31 |
| Rossmanite | $\square(LiAl_2)Al_6(Si_6O_{18})(BO_3)_3(OH)_3OH$ | 35 | 16 | 69 | 21 |
| Tavorite | $LiFe^{3+}PO_4(OH)$ | 34 | 17 | 23 | 32 |
| Eucryptite | $LiAlSiO_4$ | 27 | 18 | 9 | 18 |
| Trilithionite | $KLi_{1.5}Al_{1.5}(Si_3Al)O_{10}F_2$ | 26 | 19 | 70 | 11 |
| Fluor-elbaite | $Na(Li_{1.5}Al_{1.5})Al_6(Si_6O_{18})(BO_3)_3(OH)_3F$ | 25 | 20 | 106 | 3 |
| Manganoneptunite | $KNa_2LiMn^{2+}_2Ti_2Si_8O_{24}$ | 25 | 21 | 19 | 41 |
| Hectorite | $Na_{0.3}(Mg,Li)_3Si_4O_{10}(F,OH)_2{\cdot}nH_2O$ | 17 | 22 | 20 | – |
| Fluor-liddicoatite | $Ca(Li_2Al)Al_6(Si_6O_{18})(BO_3)_3(OH)_3F$ | 15 | 23 | 41 | 15 |
| Zabuyelite | $Li_2CO_3$ | 14 | 24 | 51 | 22 |
| Nambulite | $LiMn^{2+}_4Si_5O_{14}(OH)$ | 12 | 25 | 32 | 48 |
| Sugilite | $KNa_2Fe^{3+}_2(Li_3Si_{12})O_{30}$ | 11 | 26 | 38 | 43 |
| "Liddicoatite" | $Ca(Li_2Al)Al_6(Si_6O_{18})(BO_3)_3(OH)_3(OH)$ | 10 | 27 | 71 | 16 |
| Bityite | $CaLiAl_2(Si_2BeAl)O_{10}(OH)_2$ | 8 | 28 | 15 | 26 |
| Cryolithionite | $Na_3Al_2(LiF_4)_3$ | 8 | 29 | 14 | 39 |
| Griphite | $Ca(Mn^{2+},Na,Li)_6Fe^{2+}Al_2(PO_4)_6(F,OH)_2$ | 8 | 30 | 11 | 30 |
| Lithiophosphate | $Li_3PO_4$ | 7 | 31 | 24 | 23 |
| Sokolovaite | $CsLi_2AlSi_4O_{10}F_2$ | 7 | 32 | 87 | 12 |
| Ephesite | $NaLiAl_2(Si_2Al_2)O_{10}(OH)_2$ | 6 | 33 | 5 | 42 |
| Pezzottaite | $CsLiBe_2Al_2Si_6O_{18}$ | 6 | 34 | 76 | 52 |
| Zektzerite | $NaLiZrSi_6O_{15}$ | 6 | 35 | 42 | 73 |
| Masutomilite | $KLiAlMn^{2+}(Si_3Al)O_{10}(F,OH)_2$ | 5* | 36 | 39 | 68 |
| Norrishite | $KLiMn^{3+}_2Si_4O_{10}O_2$ | 4* | 37 | 53 | 44 |

*Note*: Source of data: Tables S1 and S2. Column 3 gives the Zipf rank, where the minerals occurring at the largest number of localities have the lowest rank (Baayen, 2001, p. 13). Column 4 ranks the minerals in order of increasing discovery date, with the minerals discovered early in the history of discovery have the lowest rank. Column 4 ranks the minerals in order of decreasing age, with the minerals reported from early in the geologic record have the lowest rank. Minerals having the same discovery date or the same age are ranked by abundance within these subsets. Dash indicates that formation of the mineral could not be dated.*Qualifies as "rare" (Hazen & Ausubel, 2016).

Li minerals includes at least one species, tancoite, found in the Archean Tanco pegmatite but nowhere else. Several minerals reported from other Archean pegmatites are found at relatively high Zipf ranks, including four minerals occurring at one to three localities in addition to tancoite (Table 4) that are not listed in Table 3 or plotted in Fig. 8 as their Zipf rank exceeds 37.

Of the five Li minerals listed in Table 4, only two have been found in post-Archean rocks, suggesting that minerals found at these distinctive localities could have formed under nearly unique conditions rarely repeated in younger pegmatites. Similarly, the distinctive conditions under which Li minerals formed in the Tip Top pegmatite, Kalahari manganese field, Pedriza massif and in four peralkaline complexes, all marked by spikes in diversity in Fig. 1c, were rarely, if ever, repeated, even from one peralkaline complex to another. Lithium minerals having a Zipf rank of 36 or higher qualify as "rare" according to Hazen & Ausubel (2016), who set the cutoff for rarity at five or fewer localities and listed four complementary causes for rarity: (1) restricted stability in *P–T–X* space; (2) essential presence of rare elements or rare combinations of elements; (3) ephemerality; and (4) human factors such as difficulty in recognition or detection because of appearance and size or occurrence in inaccessible localities, *i.e.*, human factors similar to those cited by Hystad *et al.* (2015b) to explain variations in the proportion of missing minerals (see above). Of the minerals listed in Table 4, bikitaite is an example of a

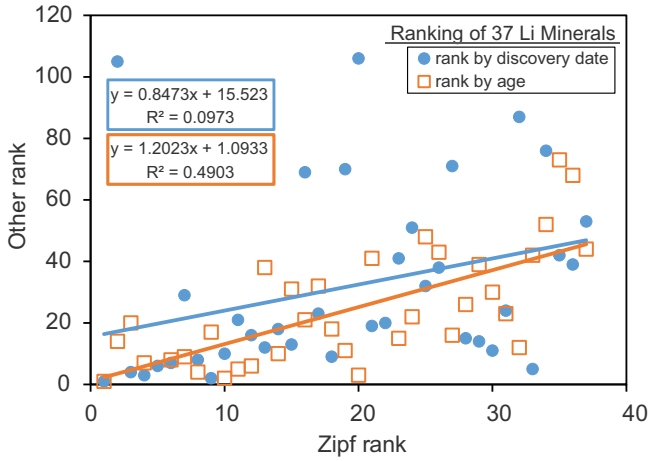


Fig. 8. Plot of discovery date rank and reported earliest occurrence rank *versus* Zipf rank based on Table 3. Minerals occurring at the largest number of localities have the lowest Zipf rank (Baayen, 2001, p. 13). Discovery dates are ranked in order of increasing discovery date, with the minerals discovered early in the history of discovery having the lowest rank. Reported earliest occurrences are ranked in order of decreasing age, with the minerals reported from early in the geologic record having the lowest rank. Minerals having the same discovery date or the same age are ranked by abundance within these subsets. The lines are linear fits with the equation and coefficient of correlation ($R^2$) given in the blue and brown boxes for discovery date and age, respectively.

Li mineral restricted in *P–T–X* conditions of formation, in this case, very low pressures and temperatures. London (1984) estimated bikitaite to form at <1.5 kbar, <200 °C by replacing the more abundant eucryptite + quartz, whereas Fasshauer *et al.* (1998) calculated <5 kbar and <300 °C, pressures and temperatures lower than those stabilizing cookeite, another more abundant mineral. Voloshinite is an example where the essential presence of a rare element is critical, in this case Rb, which is an essential constituent in only four of the 5413 currently recognized minerals. Another example is lithiowodginite, which together with lithiotantite, are the only two minerals containing essential Li and Ta. Ferroholmquistite could be an example where biased sampling contributes to its rarity because it is indistinguishable without a chemical analysis from holmquistite, which is rarely analyzed (Cámara & Oberti, 2005). Of the five minerals listed in Table 4, only tancoite lacks an obvious cause of rarity, such as rare elements, ephemerality or being unusually difficult to recognize; there is no report of its synthesis. At the only known locality, the Tanco mine, it crystallized in cavities with calcite, $Na_2HPO_4{\cdot}2H_2O$, barite and a second generation of quartz, following the formation of lithiophosphate and quartz, etching of the lithiophosphate, and apatite crystallization (Ramik *et al.*, 1980). There is no obvious reason why tancoite formed with lithiophosphate at Tanco, but in none of the other six pegmatites from which lithiophosphate is reported (Table S2). Experiments show that β–$Li_3PO_4$, the synthetic polymorph corresponding to lithiophosphate, can crystallize in aqueous solutions and is stable up to ~400 °C (atmospheric pressure), at which point it inverts to γ–$Li_3PO_4$ (Keffer *et al.*, 1967; Torres-Treviño & West, 1986). Thus, there is no significant restriction on its stability under the temperature conditions expected during pegmatite crystallization, and its occurrence in pegmatites ranging in age from 296 to 2640 Ma on five continents is no surprise. In contrast, tancoite occurs only at Tanco even though the crystal structure of tancoite has the infinite $M(TO_4)_2\Phi$ chain shared by several other minerals (Hawthorne, 1983, 1985), implying tancoite should form more easily and thus be found at more localities. Possibly it does not crystallize so readily because Li is in five-fold coordination (Hawthorne, 1983), which is less common in inorganic structures than Li in four- or six-fold coordination (*e.g.*, Wenger & Armbruster, 1991; Gagné & Hawthorne, 2016).

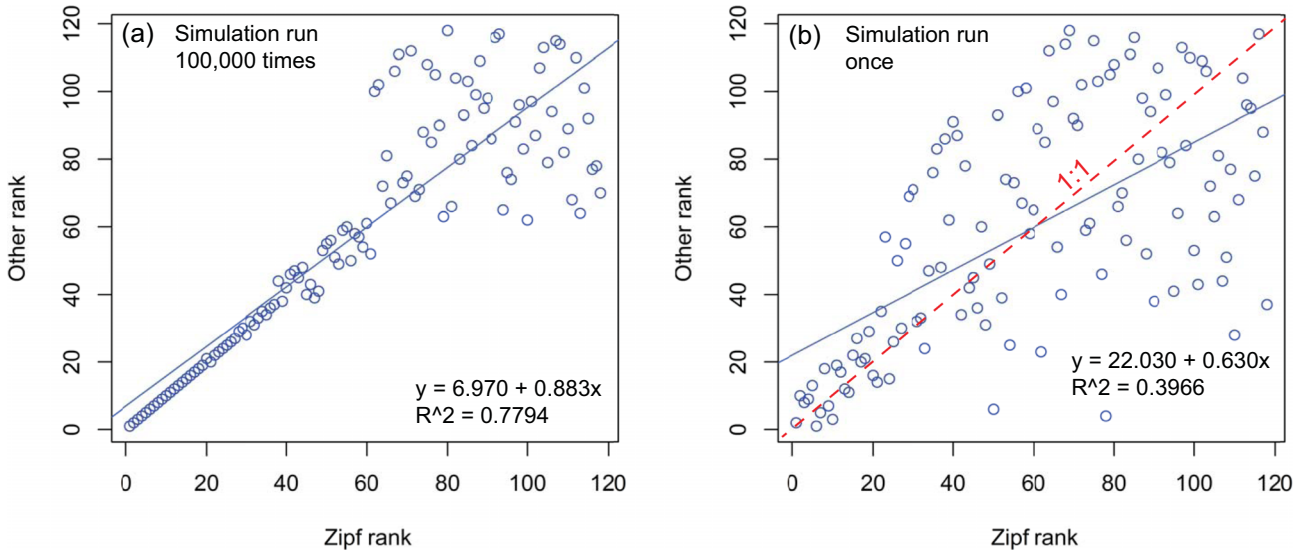


Fig. 9. Simulation of rank by discovery date or age rank (other) *versus* Zipf rank with runs of 100 000 repeats (a) or a single repeat (b) (method explained in Appendix S2). The equations and coefficient of correlation ($R^2$) are given for the solid blue lines. The red dashed line is for an ideal 1:1 ratio.

Table 4. Archean pegmatite minerals occurring at five or fewer localities.

| Mineral | Formula | Cause of rarity | Age (Ma) | Locality |
|---|---|---|---|---|
| Bikitaite | $LiAlSi_2O_6{\cdot}H_2O$ | Limited *P–T–X* | 2642 | Big Mack pegmatite, Kenora district, Ontario, Canada |
| | | | 2630 | Nolan property and Bikita pegmatite, Bikita area, Zimbabwe |
| | | | 345 | Foote Lithium company mine, Kings Mount district, North Carolina USA |
| Lithiowodginite | $LiTa_3O_8$ | Rare elements | 2640 | Tanco pegmatite, Bird River Greenstone Belt, Manitoba, Canada |
| | | | 923 | Manono mine, Katanga, Democratic Republic of Congo |
| | | | 285 | Ognevka Ta deposit, Irtysh River, Kazakhstan |
| Voloshinite | $Rb(LiAl_{1.5}\square_{0.5})(Al_{0.5}Si_{3.5})O_{10}F_2$ | Rare elements | 2660 | Red Cross Lake pegmatites, Manitoba, Canada |
| | | | Late Archean | Eastern Moblan pegmatite, Frotet-Evans greenstone belt, Quebec, Canada |
| | | | 2518 | Mt. Vasin-Myl'k, Voron'i Tundra, Kola Peninsula |
| Ferro-holmquistite | $\square Li_2(Fe^{2+}_3Al_2)Si_8O_{22}(OH)_2$ | Biased sampling | 2527 | Greenbushes Tinfield, Western Australia, Australia |
| Tancoite | $HLiNa_2[Al(PO_4)_2(OH)]$ | $^{[5]}Li(?)$ | 2640 | Tanco pegmatite, Bird River Greenstone Belt, Manitoba, Canada |

*Note*: Source of data: Tables S1 and S2. Cause of rarity (Hazen & Ausubel, 2016 except tancoite) is explained in text.

Table 5 lists the possible causes of rarity in selected examples from the 78 of 118 Li minerals occurring at five or fewer localities in post-Archean rocks. While many Li minerals have been synthesized (*e.g.*, Table S4), few experimental or theoretical studies provide the information needed for evaluation of *P–T–X* constraints on their stability as minerals. One exception is virgilite, which London (1984) showed experimentally to be stable only above 675 °C, consistent with its absence in Li-rich pegmatites, in which saturation with respect to lithium aluminosilicates is expected to occur below 675 °C. Another exception is griceite, which is closely associated with villiaumite, NaF, at Mont Saint-Hilaire, Canada (Van Velthuizen & Chao, 1989) and Dzarta Khuduk, Mongolia (Andreeva & Kovalenko, 2011), the two known localities for griceite. Villiaumite can provide constraints on the conditions of formation of griceite. Dolejš & Baker (2004; see also Dolejš & Zajacz, 2018) developed a $\mu(F_2O_{-1})$ – $\mu(Na_2O)$ diagram showing that villiaumite can be stabilized at relatively low $\mu(F_2O_{-1})$ if $\mu(Na_2O)$ is sufficiently high, *i.e.*, in peralkaline environments such as Mont Saint-Hilaire and Dzarta Khuduk. Peralkalinity *per se* is not unusual, and villiaumite is not a rare mineral (at least ten localities, *e.g.*, Anthony *et al.*, 2005). However, griceite further requires ready availability of Li. Andreeva & Kovalenko (2011) reported 1800–1900 ppm Li in the included melt hosting griceite and villiaumite and a total of 11 Li minerals have been reported from Mont Saint-Hilaire (Fig. 1c), indicating that Li was available at both localities. The combination of a peralkaline environment and ready availability of Li is relatively rare, thereby offering an explanation for the rarity of griceite. The situation with simmonsite differs from that of griceite. At the two known localities for simmonsite, Zapot pegmatite, USA (Foord *et al.*, 1999) and the Katugin massif, Russia (Sharygin & Vladykin, 2014), simmonsite is closely associated with cryolite, which Dolejš & Baker (2004) showed requires a higher $\mu(F_2O_{-1})$ albeit lower $\mu(Na_2O)$ than peralkaline environments even in the absence of the F-saturating phase, villiaumite. Cryolithionite, which is associated with simmonsite in the Zapot pegmatite, also requires high $\mu(F_2O_{-1})$ and Li availability, yet is more common (eight localities, Table S2). Thus, we suspect there could be yet another factor constraining simmonsite stability. The three minerals cryolite, simmonsite, and cryolithionite are compositionally collinear, suggesting a breakdown of simmonsite: $3Na_2LiAlF_6 \rightarrow Na_3AlF_6$ (cryolite) + $Na_3Li_3Al_2F_{12}$ (cryolithionite). However, this reaction has not been confirmed experimentally (*e.g.*, Garton & Wanklyn, 1967; Holm & Holm, 1970; Baylor *et al.* 1974; Stinton & Brown, 1975; Sabougni *et al.*, 1980). Stinton & Brown (1975) gave the most complete rendering of the subsolidus relations at one-atmosphere pressure whereby simmonsite breaks down at 543 °C to two modifications of $Na_3AlF_6$–$Li_3AlF_6$ solid solutions, whereas cryolithionite breaks down at 693 °C to one of these modifications and Na-poor $Li_3AlF_6$. In the ternary LiF–$AlF_3$–$Na_3AlF_6$ system, cryolithionite appears on the liquidus below 693 °C, but simmonsite decomposes at too low a temperature to be in equilibrium with liquid (Stinton & Brown, 1976). However, the situation is more complicated because of extensive compositional variation in cryolite and in the $Na_3AlF_6$–$Li_3AlF_6$ solid solutions, resulting in disagreement among investigators. While a plausible explanation for the rarity of simmonsite relative to cryolithionite is its lower breakdown temperature, a more

Table 5. Selected rare post-Archean Li minerals and causes of their rarity.

| Mineral | Formula | Cause of rarity | Explanation | Locality | Ref. |
|---|---|---|---|---|---|
| Virgilite | $LiAlSi_2O_6$ | Limited *P–T–X* | *T* > 675 °C; too high for pegmatite | Macusani glass, Puno department, Peru | 1 |
| Griceite | LiF | Limited *P–T–X*<br>Rare elements | Peralkalinity<br>Presence of Li | Mont Saint-Hilaire, Quebec, Canada; Dzarta Khuduk magmatic complex, Central Mongolia | 2 |
| Simmonsite | $Na_2LiAlF_6$ | limited *P–T–X* | High $\mu(F_2O_{-1})$ low breakdown temperature | Zapot pegmatite, Mineral County, Nevada, USA; Katugin deposit, Transbaikalia, Russia | 2<br>3 |
| | | Rare elements | Presence of Li | | |
| Lavinskyite | $K(LiCu)Cu_6(Si_4O_{11})_2(OH)_4$ | Rare elements | Presence of Li + Cu | Wessels mine, Kalahari manganese field, South Africa; Cerchiara mine, Eastern Liguria, Italy | 4 |
| Balestraite | $KLi_2V^{5+}Si_4O_{12}$ | Rare elements | Presence of Li + V | Cerchiara mine, Eastern Liguria, Italy | 4 |
| Watatsumiite | $KNa_2LiMn_2V_2Si_8O_{24}$ | Rare elements | Presence of Li + V | Tanohata mine, Iwate prefecture, Japan | 5 |
| Hsianghualite | $Li_2Ca_3Be_3(SiO_4)_3F_2$ | Rare elements | Presence of Li + Be in a skarn mineral | Xianghualing ore field, Hunan Province, China | 6 |
| Liberite | $Li_2Be(SiO_4)$ | Rare elements | Presence of Li + Be in a skarn mineral | Xianghualing ore field, Hunan Province, China | 6 |
| Nanlingite | $Na(Ca_5Li)Mg_{12}(AsO_3)_2[Fe^{2+}(AsO_3)_6]F_{14}$ | Rare elements | Presence of Li + As | Xianghualing ore field, Hunan Province, China | 7 |
| Walkerite | $Ca_{16}(Mg,Li)_2[B_{13}O_{17}(OH)_{12}]_4Cl_6{\cdot}28H_2O$ | Ephemeral | Drill core | Penobsquis potash deposit, New Brunswick, Canada | 8 |
| Jadarite | $LiNaB_3SiO_7(OH)$ | Ephemeral | Drill core | Borehole, Jadar Basin, western Serbia | 9 |
| Tiptopite | $K_2(Li,Na,Ca)_6(Be_6P_6)O_{24}(OH)_2{\cdot}1.3H_2O$ | – | – | Tip Top mine, Custer County, South Dakota USA | 10 |

Sources of data: Table S1 and S2; References 1. London (1984); 2. Dolejš & Baker (2004), Dolejš & Zajacz (2018); 3. Stinton & Brown (1975, 1976); 4. Kolitsch *et al.* (2018); 5. Matsubara *et al.* (2003); 6. Rao *et al.* (2017); 7. Yang *et al.* (2011); 8. Grice *et al.* (2002); 9. Stanley *et al.* (2007); 10. Grice *et al.* (1985). Cause of rarity (Hazen & Ausubel, 2016) is explained in text.

quantitative explanation would require a better understanding of the subsolidus relations in the $Na_3AlF_6$–$Li_3AlF_6$ binary system, particularly at pressures greater than one atmosphere.

A more common cause of rarity is the unusual combinations of elements not normally enriched together such as Li + V and Li + Cu in balestraite, lavinskyite and watatsumiite in metasomatized manganese deposits, both oxidized ($V^{5+}$, $Mn^{3+}$, $Fe^{3+}$, Kolitsch *et al.*, 2018) and mildly reduced ($V^{4+}$, $Mn^{2+}$, $Fe^{2+}$, Matsubara *et al.*, 2003, Table 5). Another example is the rarity of skarn minerals containing both Li and Be as essential constituents, such as hsianghualite and liberite. Although Li can be present in Be-rich skarns, typically as a constituent of mica (Ginzburg, 1975; Barton & Young, 2002), its concentration in Be-rich skarns rarely suffices for a Li-rich mineral other than mica to form. Jadarite and walkerite are ephemeral minerals found only in drill core in association with evaporite deposits; difficulty of access could also be contributing to their rarity. However, the rarity of tiptopite remains unexplained; it occurs along fracture surfaces in beryl, less commonly in quartz and microcline perthite, an environment often encountered in pegmatites, yet the reported occurrence of tiptopite was restricted to just one area in the Tip Top mine in South Dakota (Grice *et al.*, 1985). In summary, we can conclude from this selection of Archean and post-Archean examples, that rarity, and by extension, diversity, can be readily explained in many cases as suggested by Hazen & Ausubel (2016), and thus their rare occurrence is considered deterministic.

This observation brings us back to the conclusion reached by Hazen *et al.* (2015a) that "much of Earth's mineral diversity associated with rare species results from stochastic processes", *i.e.*, most rare minerals "arise only in a restricted environment with an improbable combination of physical and geochemical conditions—environments that may occur on only a small fraction of all terrestrial planets" (Hazen, 2017). We need to reconcile these two perspectives on mineral rarity and diversity by clarifying just what is meant by "stochastic", which has been used differently in different branches of science. The use by biologists to characterize the various factors acting on species in ecological communities is perhaps the most appropriate analogy in considering mineral assemblages in mineral ecology. For example, in regard to ecological stochasticity, Zhou & Ning (2017) wrote that "in contrast to deterministic processes, here, stochastic processes are referred to as ecological processes that generate community diversity patterns indistinguishable from those generated by random chance alone" and "a process is considered stochastic (or random) with respect to a

certain reference status if the outcome is probabilistic." That chance plays the key role in stochastic processes was also emphasized by Blount *et al.* (2018). Distinguishing between deterministic and stochastic processes in studies of animal and plant communities has proven to be a challenge to biologists, who have deployed sophisticated statistical techniques to make the distinction. Nonetheless, in numerous cases, deterministic processes are found to be predominant (*e.g.*, Benedetti-Cecchi *et al.*, 2015). If an analogy can be drawn with biological communities, mineral assemblages could also be regarded as a product of both deterministic and stochastic processes, and the former could be dominant. On the scale of individual species, two of the causes cited by Hazen & Ausubel (2016) for mineral rarity, *P–T–X* conditions and rarity of essential elements, are deterministic, implying that the mineral assemblages from which the minerals listed in Tables 4 and 5 originated are largely the result of deterministic processes. On the scale of the geological formations in which Li minerals are found, for example, Li-rich granitic pegmatites, London & Morgan (2017) reported success in experimentally reproducing seven features of such pegmatites, including feldspathic outer zones and quartz-rich cores and albite + lepidolite bodies as the latest primary assemblage, suggesting crystallization of pegmatites is largely a deterministic process. And at the planetary scale, we again see a major role played by deterministic processes, *e.g.*, the processes whereby Li is redistributed in a subduction zone and recycled residual crust acquires an isotopically light signature (Elliott *et al.*, 2004).

Overall, 83 Li minerals are rare, occurring at five localities or fewer, resulting in a distribution of Li minerals in Earth's crust that is far from random. The probability of finding these rare minerals is much less than the probability of finding the common and widespread Li minerals such as spodumene, elbaite, or triphylite. This non-random distribution is analogous to the "intratextural differences", *i.e.*, non-random distributions, which Baayen (2001, p. 34) warned could be a complicating factor in comparing two different written texts. Hystad *et al.* (2019) found that a zero-truncated Poisson-lognormal distribution provides the best fit to the mineral frequency distribution using Bayesian methods and that this modeling gave more reasonable estimates for the population size. However, this model still assumes randomness, which is one of its weaknesses. Moreover, can such models inform us about the geologic processes in the past which resulted in the present-day non-random distribution?

An analogous situation is faced by linguists, biologists and other scientists in understanding why language and other systems obey Zipf's law, which states that when observations "are ranked by the frequency of their occurrence, the frequency of a particular observation is inversely proportional to its rank" (Aitchison *et al.*, 2016). These authors pointed out that underlying causes, not Zipf's law itself, could provide insight into statistical regularities in a wide range of fields of study. In a review of the literature on the application of Zipf's law in linguistics, Piantadosi (2014) concluded that to make progress at understanding why language obeys Zipf's law, studies must seek evidence beyond the law itself, based on "new, independent data." Piantadosi (2014) added that many studies try to explain the Zipfian distribution instead of uncovering the causal forces that drive word frequencies, and do not account for any psychological processes of word production, especially the intentional choice of words in order to convey a desired meaning. Piantadosi (2014) concluded linguists should focus on explaining what words are needed at each juncture in a conversation – this effort could elucidate why word frequencies look the way they do. By analogy, mineralogists should not seek explanations in LNRE models for the observed distribution of minerals, but continue to use the geologic history, mineralogical data, and known distributions, *i.e.*, Piantadosi's (2014) "new, independent data", to explain Zipfian distribution. Thus, it seems unlikely that LNRE models can meaningfully inform us about Earth's geological history. Quite the contrary, the non-random distribution of minerals in Earth's crust at the present time could complicate comparison of Earth's current mineral endowment with an Earth-like planet or with "replaying the tape" of Earth's mineral evolution through geologic history. Baayen (2001, p. 34) warned that in comparing two texts, the *intertextural* differences must exceed the *intratextural* differences for the comparison to be meaningful. This distinction may be difficult to evaluate as so little would be known about mineral distributions on another planet, including Mars, or on the "replayed" Earth.

Baayen (2001, p. 34) raised a second issue – word frequency distributions are impacted by size of the text, and comparisons between texts differing "substantially" in size can be problematic. The same caveat can be applied to comparison of Earth with Earth-like planets. Hystad *et al.* (2019) generated two random samples of size $N = 652\,856$ mineral/locality pairs to estimate the expected number of species that would be different, and obtained about 16% using the Poisson-lognormal distribution (Hystad *et al.*, 2017, used a similar approach, but with the Sichel GIGP distribution). Applying this estimate to the comparison of two modeled Earth-like planets assumes N is the same for both. At present, the number of mineral/locality counts on the nearest celestial objects, namely the Moon, Mars, asteroid bodies, either through direct sampling or from meteorites originating on these celestial bodies, probably number at most in the hundreds, even counting areas micrometers in scale as distinct localities such as the individual Ca–Al-rich inclusions in the Allende carbonaceous chondrite described by Chi Ma and his colleagues (*e.g.*, Ma *et al.*, 2014). Thus, there are too few mineral/locality counts on any one of these celestial bodies for a meaningful experimental test of the 16% estimate for the proportion of different minerals: the sample sizes for Earth and any one of these celestial bodies differ by at least three orders of magnitude.

We can now return to the question raised earlier whether LNRE models can inform us both about the history of discovery (human factors) and Earth's geological history. One could view the interplay between these two histories as potentially operating in two directions: (1) information on geologic history and mineral evolution can inform LNRE

modeling, and (2) information contained in the LNRE modeling can inform about the geologic history and mineral evolution. Figure 8 shows the poor correspondence between the Zipf rank on the one hand and the date of discovery and reported age of earliest occurrence in the geologic record on the other, which can be attributed to geological as well as human factors. In other words, the non-random distribution of minerals in Earth's crust contributes to differences in the probabilities among species being discovered, which has a profound impact on LNRE modeling, just as non-random distribution of words in a text affects modeling of word frequency in the text. However, as emphasized by Piantadosi (2014) in his review of linguistic studies, making progress in understanding why distribution of minerals can be modeled, we must seek evidence beyond the model itself, using geologic and mineralogical data, that is, LNRE models do not inform us about Earth's geological history, and the interplay does not operate in two directions. When comparing Earth with Earth-like planets or in considering a replay of Earth's tape, we need to keep in mind not only the complexities introduced by the non-random distribution of minerals, but also size of the sample modeled, since substantial differences in sample size can also invalidate such comparisons.

## 6. Conclusions

Based on locality data and ages of formation of 118 Li minerals (as of early 2018), a cumulative diversity diagram (Fig. 1b) and a histogram giving estimates of the number of minerals formed in a given 50 million year interval (Fig. 1c) show that throughout the Precambrian increases in Li mineral diversity are related to supercontinent assembly (or to supercraton assembly in the Late Archean, according to Bleeker, 2003) and growth of juvenile continental crust, whereas preservation bias undoubtedly contributes substantially to the surge in diversity in the Phanerozoic, as do localities of unusual diversity such as peralkaline igneous complexes. Similar features are displayed in the corresponding diagrams for Be minerals (Grew & Hazen, 2014) and B minerals (Grew, 2017; Grew *et al.*, 2016). These diagrams provide support for the overall concept of mineral evolution that Earth's mineralogy in the past differed from today's mineralogy and that changes are related to other geologic phenomena.

A different set of diagrams (Figs. 2, 3, 7a) illustrates the history of human discovery of Li minerals. The surge of discoveries of Li minerals in the last 30 years is almost entirely due to finding structural analogs that constitute 75% of Li minerals; revisions in nomenclature, particularly in the tourmaline and amphibole supergroups, have allowed for finer distinctions between species based on occupancy of crystallographic sites. As only 13 Li minerals were synthesized prior to their discovery in nature, it is unlikely synthetic compounds will be a promising source for predicting potential new Li minerals.

Zero truncated Poisson-lognormal distribution using Bayesian methods, which was found to provide the best fit to mineral frequency distribution (Hystad *et al.*, 2019), indicate that estimates of total species are accompanied by greater uncertainties for Li, B, and Be minerals treated as individual subsets than for all minerals. The total median population estimated for the B data obtained through 2017 is nearly double that for the B data obtained through 1978 (Table 1), a discrepancy most likely due to advances in analytical technology as argued by Grew *et al.* (2017a). Since further technological advances are likely, the total population estimated from the 2017 data is also likely to be an underestimate, and thus the upper range of the 95% posterior interval, *i.e.*, 1200–1500 B species, might be the better estimate for the total population of B minerals. Corresponding estimates for Li and Be minerals range from ~700–~800 species. The totality of mineral species, at least for subsets numbering a few hundred species, like the totalities of biological species, may remain conjectural for some time to come.

The Li minerals reported from the largest number of localities (low Zipf rank) would be expected to be discovered earliest in the historic search for new minerals (Fig. 7a), and due to their greater abundance, we might expect that they would also have appeared earliest in the Earth's history (Fig. 1b). However, scatter in Fig. 8 implies that factors other than number of present-day localities (Zipf rank) play a role in mineral ecology. More significant are the unique formation conditions at a handful of localities that produced a diverse suite of Li minerals rarely, if ever, found elsewhere (*e.g.*, Table 4). The resulting non-random distribution of minerals in present-day Earth's crust contributes significantly to differences in the probabilities among species of being discovered, which can have a profound impact on LNRE modeling.

Having estimated Earth's total mineral endowment using LNRE and related modeling, can we consider implications for the mineral endowment of Earth-like planets, or the thought experiment of "replaying the tape" of mineral evolution in Earth history? LNRE and related ecological modeling of Earth's present mineral endowment reflects the human history of mineral discovery as well as mineral evolution up to the present time in Earth history. To better understand and apply ecological models of mineral distribution, we must take into account historical factors in mineral discovery, geological evidence of mineral evolution over time, and the stochastic and deterministic factors influencing mineral occurrence.

**Acknowledgements:** This paper is dedicated to Christian Chopin in recognition for his over 30 years of service as Managing Editor of the *European Journal of Mineralogy*. Christian has been a responsive correspondant and has been generous in his sharing of critical scientific information. His meticulous editing has greatly contributed to the reputation of the journal.

The Interlibrary Loan service at the Fogler Library, University of Maine and the IMA Database of Mineral Properties maintained by the RRUFF Project at the University of

Arizona (Lafuente *et al.*, 2015) provided access to the literature essential for carrying out this research.
The following individuals are thanked for their generous contribution of critical information either unpublished or not otherwise readily accessible that was critical to compiling the locality data on which much of this paper is based (Tables S1 and S2): Raquel Alonso-Perez for attempts to identify possible swinefordite in the Harvard collection from the Gem Star mine, California, USA; Chris Carson for information on the age of pegmatite containing griphite from Northern Territory, Australia; Nikita Chukanov for information on sugilite from South Africa; Christian Chopin for information on ephesite from Val Gilba, Italy; Marco Ciriotti for information on several Italian minerals; Giancarlo Della Ventura for information on possible nambulite from the Molinello mine, Italy; Alla Dolgopolova for a preliminary age on the Verkhnee Espe deposit, Kazakhstan; Guillaume Estrade for unpublished information on zektzerite in the Ambohimirahavavy complex, Madagascar; Andreas Ertl for information and samples of mica reported to be ephesite from Amstall and Wolfsbach in Lower Austria; Joseph M. Evensen for an unpublished analysis of Li mica from the Harding Mine, New Mexico, USA; Guang Fan for translations and papers giving the ages of pegmatites where luanshiweiite occurs; Shah Wali Faryad on possible nambulite from Čierna Mine, Slovakia; Stephen Guggenheim for information on bityite and other Li micas; Frank Hawthorne for information on ferri-leakeite from the Hoskins mine, Australia, and for drawing our attention to the five-fold coordination of Li in tancoite; Vladimir Karpenko for information (in part unpublished) on tainiolite and neptunite from Darai Pioz and ages of pegmatites in the Alai Range, Tajikistan; Pavel M. Kartashov for information on his reports of ferro-ferri-fluoro-leakeite from the Khaldzan Buragtag massif, Mongolia, lithiotantite and lithiowodginite from Manono Mine, Katanga, and swinefordite from Kenticha mine, Ethiopia; Irina I. Kupryanova for information on the names of specific localities for Be minerals cited in Ginzburg's (1975) book (Appendix S1); Joseph Meert for information on the age of the Kajlidongri Mine, Madhya Pradesh, India and on the Aravalli Supergroup, India; Mariko Nagashima for information on pyroxenoids related to nambulite; Roberta Oberti for information on Li amphiboles; Igor Pekov for information on the report of bityite from Pitkyaranta, Karelia, Russia and for assistance in obtaining information on bityite, ephesite and other minerals from the former U.S.S.R.; Federico Pezzotta for information on occurrences of several minerals in Italy; Dingyi Qian for translations of critical Chinese texts; Mike Rumsey for information on sugilite from the Central Provinces of India; Can Rao for information on nanlingite from the Xianghualing skarn, China, and on other minerals found in China; William B. Simmons, Jr. for unpublished data on griphite from Animikie Red Ace pegmatite, Wisconsin, USA; Rainer Thomas for unpublished information on cryolithionite and zabuyelite as daughter crystals in fluid inclusions; Martin G. Yates for unpublished electron microprobe analyses of micas from Lower Austria.
We are particularly grateful to Priscilla C. Grew for fruitful discussions on the relationship of LNRE modeling to the human history of discovering new minerals and on the relative roles of stochastic and deterministic processes in the formation of minerals.
We thank two anonymous reviewers and Wouter Bleeker for their thoughtful and constructive comments on the first version of the manuscript, as well as Associate Editor Thomas Armbruster, who handled the manuscript and commented on it.
Hazen's studies in mineral ecology are supported in part by the Deep Carbon Observatory, the Alfred P. Sloan Foundation, the W.M. Keck Foundation, the John Templeton Foundation, a private foundation, and the Carnegie Institution for Science. Ongoing studies in mineral evolution and ecology have benefitted from discussions with and suggestions by Robert Downs, Olivier Gagné Daniel Hummer, Sergey Krivovichev, Chao Liu, and Shaunna Morrison.

## Note added in proof

Pimm & Jenkins (2019) in a diagram on page 164 show that bird species having a larger geographic range tended to be discovered earlier than birds having a smaller geographic range. This relationship is analogous to that in Fig. 8, which shows Li minerals occurring at more localities (low Zipf rank) tended to be discovered earlier than Li minerals occurring at fewer localities (high Zipf rank).

## References

Agusdinata, D.B., Liu, W., Eakin, H., Romero, H. (2018): Socio-environmental impacts of lithium mineral extraction: towards a research agenda. *Environ. Res. Lett.*, **13**, 123001. https://doi.org/10.1088/1748-9326/aae9b1.

Aitchison, L., Corradi, N., Latham, P.E. (2016): Zipf's law arises naturally when there are underlying, unobserved variables. *PLoS Comput. Biol.*, **12** (12), e1005110. https://doi.org/10.1371/journal.pcbi.1005110.

Andreeva, I.A. & Kovalenko, V.I. (2011): Evolution of the trachydacite and pantellerite magmas of the bimodal volcanic association of Dzarta-Khuduk, central Mongolia: investigation of inclusions in minerals. *Petrology*, **19**, 348–369.

Anthony, J.W., Bideaux, R.A., Bladh, K.W., Nichols, M.C. eds (2005): Villiaumite in handbook of mineralogy. Mineralogical Society of America, Chantilly, USA. http://www.handbookofmineralogy.org/.

Arfwedson, J.A. (1818): Undersökning af några vid Utö Jernmalmsbrott förekommande Fossilier, och af ett deri sunnet eget Eldfast Alkali. *Afhandlingar Fysik, Kemi Mineral.*, **6**, 145–176. (in Swedish).

Baayen, R.H. (2001): Word frequency distributions. Kluwer, Dordrecht, The Netherlands, 333 p.

Back, M.E. (2014): Fleischer's glossary of mineral species 2014. The Mineralogical Record Inc., Tucson, Arizona, 410 p.

Bailey, S.W. (1980): Summary of recommendations of AIPEA Nomenclature Committee. *Am. Mineral.*, **65**, 1–7.

Barton, M.D. & Young, S. (2002): Non-pegmatitic deposits of beryllium: mineralogy, geology, phase equilibria and origin. in "Beryllium: mineralogy, petrology, and geochemistry", E.S. Grew, ed., Reviews in mineralogy and geochemistry.

Mineralogical Society of America Chantilly, Virginia, **50**, 591–691.

Baylor, R. Jr., Stinton, D.P., Brown, J.J. (1974): Subsolidus equilibria in the system LiF-$AlF_3$-$Na_3A1F_6$. *J. Am. Ceram. Soc.*, **57**, 470–471.

Benedetti-Cecchi, L., Canepa, A., Fuentes, V., Tamburello, L., Purcell, J.E., Piraino, S., Robert, J., Boero, F., Halpin, P. (2015): Deterministic factors overwhelm stochastic environmental fluctuations as drivers of jellyfish outbreaks. *PLoS One*, **10** (10), e0141060. https://doi.org/10.1371/journal.pone.0141060.

Berzelius, J.J. (1818): Ein neues mineralisches Alkali und ein neues Metall. *J. Chem. Phys.*, **21**, 44–48.

Bleeker, W. (2003): The late Archean record: a puzzle in *ca.* 35 pieces. *Lithos*, **71**, 99–134.

Bleeker, W., Chamberlain, K.R., Kamo, S.L., Hamilton, M., Kilian, T.M., Buchan, K.L. (2016): Kaapvaal, Superior and Wyoming: nearest neighbours in supercraton Superia. *in* "International Geological Congress, Abstracts, 35, Abstract 5222".

Blount, Z.D., Lenski, R.E., Losos, J.B. (2018): Contingency and determinism in evolution: replaying life's tape. *Science* **362**, eaam5979, 1–10. https://doi.org/10.1126/science.aam5979.

Cámara, F. & Oberti, R. (2005): The crystal-chemistry of holmquistites: ferroholmquistite from Greenbushes (Western Australia) and hints for compositional constraints in $^{B}$Li amphiboles. *Am. Mineral.*, **90**, 1167–1176.

Campbell, T.J. & Roberts, W.L. (1986): Phosphate minerals from the Tip Top mine, Black Hills, South Dakota. *Mineral. Record*, **17**, 237–254.

Černý, P. (2005): The Tanco rare-element pegmatite deposit, Manitoba: Regional context, internal anatomy, and global comparisons. *in* "Rare-element geochemistry and mineral deposits", R.L. Linnen, I.M. Samson, eds., GAC short course notes. Geological Association of Canada, 127–158.

Chopin, C., Goffé, B., Ungaretti, L., Oberti, R. (2003): Magnesiostaurolite and zincostaurolite: mineral description with a petrogenetic and crystal-chemical update. *Eur. J. Mineral.*, **15**, 167–176.

Clay Minerals Society (2019): The clay minerals society glossary of clay science. The Clay Minerals Society, Chantilly, VA.

Dolejš, D. & Baker, D.R. (2004): Thermodynamic analysis of the system $Na_2O$–$K_2O$–CaO–$Al_2O_3$–$SiO_2$–$H_2O$–$F_2O_{-1}$: stability of fluorine-bearing minerals in felsic igneous suites. *Contrib. Mineral. Petrol.*, **146**, 762–778.

Dolejš, D. & Zajacz, Z. (2018): Halogens in silicic magmas and their hydrothermal systems. *in* "The role of halogens in terrestrial and extraterrestrial geochemical processes", D.E. Harlov, L. Aranovich, eds., Geochemistry. Springer, 431–543.

Elliott, T., Jeffcoate, A., Bouman, C. (2004): The terrestrial Li isotope cycle: light-weight constraints on mantle convection. *Earth Planet. Sci. Lett.*, **220**, 231–245.

Fasshauer, D.W., Chatterjee, N.D., Cemic, L.C. (1998): A thermodynamic analysis of the system $LiAlSiO_4$-$NaAlSiO_4$-$Al_2O_3$-$SiO_2$-$H_2O$ based on new heat capacity, thermal expansion, and compressibility data for selected phases. *Contrib. Mineral. Petrol.*, **133**, 186–198.

Fersman, A.E. (1938): On the number of mineral species. *C. R. (Doklady) Acad. Sci. URSS*, **19**, 269–272.

Foord, E.E., O'Connor, J.T., Hughes, J.M., Sutley, S.J., Falster, A.U., Soregaroli, A.E., Lichte, F.E. (1999): Simmonsite, $Na_2LiAlF_6$, a new mineral from the Zapot amazonite-topaz-zinnwaldite pegmatite, Hawthorne, Nevada, U.S.A. *Am. Mineral.*, **84**, 769–772.

Gagné, O.C. & Hawthorne, F.C. (2016): Bond-length distributions for ions bonded to oxygen: alkali and alkaline-earth metals. *Acta Crystallogr.*, **B72**, 602–625.

Garton, G. & Wanklyn, B.M. (1967): Reinvestigation of the system $Na_3A1F_6$-$Li_3A1F_6$. *J. Am. Ceram. Soc.*, **50**, 395–399.

Ginzburg, A.I. ed (1975): Genetic types of hydrothermal beryllium deposits. Nedra, Moscow, Russia, 247 p. (in Russian).

Gould, S.J. (1989): Wonderful life. The Burgess shale and the nature of history. Norton, New York, NY.

Grew, E.S. (2017): Boron: from cosmic scarcity to 300 minerals. *Elements*, **13**, 225–229.

Grew, E.S. & Hazen, R.M. (2014): Beryllium mineral evolution. *Am. Mineral.*, **99**, 999–1021.

Grew, E.S., Dymek, R.F., De Hoog, J.C.M., Harley, S.L., Boak, J. M., Hazen, R.M., Yates, M.G. (2015): Boron isotopes in tourmaline from the *ca.* 3.7-3.8 Ga Isua supracrustal belt, Greenland: sources for boron in Eoarchean continental crust and seawater. *Geochim. Cosmochim. Acta*, **163**, 156–177.

Grew, E.S., Krivovichev, S.V., Hazen, R.M., Hystad, G. (2016): Evolution of structural complexity in boron minerals. *Can. Mineral.*, **54**, 125–143.

Grew, E.S., Hystad, G., Hazen, R.M., Golden, J., Krivovichev, S.V., Gorelova, L.A. (2017a): How many boron minerals occur in Earth's upper crust? Invited Centennial Paper. *Am. Mineral.*, **102**, 1573–1587.

Grew, E.S., Hystad, G., Hazen, R.M., Krivovichev, S.V., Golden, J.J. (2017b): Estimating Earth's endowment of beryllium minerals: insight from counting boron minerals, 213–215. RMS-DPI code 2017-1-244-1. Permanent address of publication: http://www.minsoc.ru/2017-1-244-1/.

Grew, E.S., Bosi, F., Rios, L., Kristiansson, P., Gunter, M.E., Hålenius, U., Trumbull, R.B., Yates, M.G. (2018a): Fluorelbaite, lepidolite and Ta–Nb oxides from a pegmatite of the 3000 Ma Sinceni Pluton, Swaziland: evidence for lithium–cesium–tantalum (LCT) pegmatites in the Mesoarchean. *Eur. J. Mineral.*, **30**, 205–218.

Grew, E.S., Hystad, G., Ostroverkhova, A., Golden, J.J., Krivovichev, S.V., Hazen, R.M. (2018b): Can lithium minerals be counted? Comparison with boron and beryllium. *in* "XXII Meeting of the International Mineralogical Association, 13-17 August 2018, Melbourne. Book of Abstracts", 180 p.

Grice, J.D., Peacor, D.R., Robinson, G.W., Van Velthuizen, J., Roberts, W.L., Campbell, T.J., Dunn, P.J. (1985): Tiptopite (Li, K,Na,Ca,□)$_8$$Be_6$$(PO_4)_6$$(OH)_4$, a new mineral species from the Black Hills, South Dakota. *Can. Mineral.*, **23**, 43–46.

Grice, J.D., Gault, R.A., Van Velthuizen, J., Pratt, A. (2002): Walkerite, a new borate mineral species in an evaporitic sequence from Sussex, New Brunswick, Canada. *Can. Mineral.*, **40**, 1675–1686.

Guggenheim, S., Adams, J.M., Bain, D.C., Bergaya, F., Brigatti, M.F., Drits, V.A., Formoso, M.L.L., Galán, E., Kogure, T., Stanjek, H. (2006): Summary of recommendations of nomenclature committees relevant to clay mineralogy: report of the Association Internationale pour l'Etude des Argiles (AIPEA) Nomenclature Committee for 2006. *Clays Clay Minerals*, **54**, 761–772.

Güven, N. (1988): Smectites. *in* "Hydrous phyllosilicates (exclusive of micas)", S.W. Bailey, ed., Reviews in mineralogy. Mineralogical Society of America, Chantilly, Virginia, **19**, 497–559.

Hålenius, U., Hatert, F., Pasero, M., Mills, S. (2018): Mineral diversity: beyond 7000 species? *in* "XXII Meeting of the International Mineralogical Association, 13-17 August 2018, Melbourne". Book of Abstracts. 356 p.

Harris, P.D., Robb, L.J., Tomkinson, M.J. (1995): The nature and structural setting of rare-element pegmatites along the northern flank of the Barberton greenstone belt, South Africa. *South Afr. J. Geol.*, **98**, 82–94.

Hawkesworth, C., Cawood, P., Dhuime, B. (2013): Continental growth and crustal record. *Tectonophysics*, **609**, 651–660.

Hawthorne, F.C. (1983): The crystal structure of tancoite. *Tschermaks Mineral. Petrograph. Mitt.*, **31**, 121–135.

— (1985): Towards a structural classification of minerals: the $^{VI}M^{IV}T_2\Phi_n$ minerals. *Am. Mineral.*, **70**, 455–473.
Hawthorne, F.C., Oberti, R., Harlow, G.E., Maresch, W.V., Martin, R.F., Schumacher, J.C., Welch, M.D. (2012): Nomenclature of the amphibole supergroup. *Am. Mineral.*, **97**, 2031–2045.
Hazen, R.M. (2017): Chance, necessity and the origins of life: a physical sciences perspective. *Phil. Trans. R. Soc. A*, **375**, 20160353. https://doi.org/10.1098/rsta.2016.0353.
Hazen, R.M. & Ausubel, J.H. (2016): On the nature and significance of rarity in mineralogy. *Am. Mineral.*, **101**, 1245–1251.
Hazen, R.M., Papineau, D., Bleeker, W., Downs, R.T., Ferry, J.M., McCoy, T.J., Sverjensky, D.A., Yang, H. (2008): Mineral evolution. *Am. Mineral.*, **93**, 1693–1720.
Hazen, R.M., Golden, J., Downs, R.T., Hystad, G., Grew, E.S., Azzolini, D., Sverjensky, D.A. (2012): Mercury (Hg) mineral evolution: a mineralogical record of supercontinent assembly, changing ocean geochemistry, and the emerging terrestrial biosphere. *Am. Mineral.*, **97**, 1013–1042.
Hazen, R.M., Grew, E.S., Downs, R.T., Golden, J., Hystad, G. (2015a): Mineral ecology: chance and necessity in the mineral diversity of terrestrial planets. *Can. Mineral.*, **53**, 295–324.
Hazen, R.M., Hystad, G., Downs, R.T., Golden, J., Pires, A., Grew, E.S. (2015b): Earth's "missing" minerals. *Am. Mineral.*, **100**, 2344–2347.
Hazen, R.M., Hystad, G., Downs, R.T., Eleish, A., Morrison, S.M. (2018): A revised (upwards) estimate of Earth's "missing" minerals. *in* "XXII Meeting of the International Mineralogical Association, 13-17 August 2018, Melbourne. Book of Abstracts", 181 p.
Henry, D.J., Novák, M., Hawthorne, F.C., Ertl, A., Dutrow, B.L., Uher, P., Pezzotta, F. (2011): Nomenclature of the tourmaline-supergroup minerals. *Am. Mineral.*, **96**, 895–913.
Hoffman, P.F. (1997): Tectonic genealogy of North America. *in* "Earth structure: an introduction to structural geology and tectonics", B.A. van der Pluijm, S Marshak, eds. McGraw-Hill, New York, NY, 459–464 pp.
Holm, J.L. & Holm, B.J. (1970): Phase investigations in the system $Na_3A1F_6$-$Li_3A1F_6$. *Acta Chem. Scand.*, **24**, 2535–2545.
Hommels, C.H., Saat, T.A.W., Kuiper, P.J.C. (1990): Characterization of the high-affinity $K^+(Rb^+)$-uptake system in roots of intact Taraxacum microspecies: comparison of 12 microspecies in relation to their mineral ecology. *New Phytot.*, **114**, 695–701.
Horváth, A. & Gault, R.A. (1990): The mineralogy of Mont Saint-Hilaire, Quebec. *Mineral. Record*, **21**, 284–359.
Hystad, G., Downs, R.T., Hazen, R.M. (2015a): Mineral frequency distribution data conform to a LNRE model: prediction of Earth's "missing" minerals. *Math. Geosci.*, **47**, 647–661.
Hystad, G., Downs, R.T., Grew, E.S., Hazen, R.M. (2015b): Statistical analysis of mineral diversity and distribution: Earth's mineralogy is unique. *Earth Planet. Sci. Lett.*, **426**, 154–157.
Hystad, G., Downs, R.T., Hazen, R.M., Golden, J.J. (2017): Relative abundances of mineral species: a statistical measure to characterize earth-like planets based on earth's mineralogy. *Math. Geosci.*, **49**, 179–194.
Hystad, G., Eleish, A., Hazen, R.M., Morrison, S.H., Downs, R.T. (2019): Bayesian estimation of Earth's undiscovered mineralogical diversity using noninformative priors. *Math. Geosci.*, **51**, 401–417. https://doi.org/10.1007/s11004-019-09795-8.
Jones, A.A. & Bennett, P.C. (2017): Mineral ecology: surface specific colonization and geochemical drivers of biofilm accumulation, composition, and phylogeny. *Front. Microbiol.*, **8**, 491. https://doi.org/10.3389/fmicb.2017.00491.
Keffer, C., Mighell, A.D., Mauer, F., Swanson, H., Block, S. (1967): The crystal structure of twinned low-temperature lithium phosphate. *Inorganic Chem.*, **6**, 119–125.
Kolitsch, U., Merlino, S., Belmonte, D., Carbone, C., Cabello, R., Lucchetti, G., Ciriotti, M.E. (2018): Lavinskyite-1*M*, K(LiCu)$Cu_6(Si_4O_{11})_2(OH)_4$, the monoclinic MDO equivalent of lavinskyite-2*O* (formerly lavinskyite), from the Cerchiara manganese mine, Liguria, Italy. *Eur. J. Mineral.*, **30**, 811–820.
Lafuente, B., Downs, R.T., Yang, H., Stone, N. (2015): The power of databases: the RRUFF project. *in* "Highlights in mineralogical crystallography", T. Armbruster, R.M. Danisi, eds. W. De Gruyter, Berlin, Germany, 1–30.
Larsen, A.O., ed (2010): The Langesundfjord. History, Geology, Pegmatites, Minerals. Bode Verlag, Salzhemmendorf, Germany.
Loomis, T.A. & Campbell, T.J. (2002): The Tip Top pegmatite: a historical review and mineralogical update. *Matrix*, **10**, 138–146.
London, D. (1984): Experimental phase equilibria in the system $LiAlSiO_4$—$SiO_2$—$H_2O$: a petrogenetic grid for lithium-rich pegmatites. *Am. Mineral.*, **69**, 995–1004.
London, D. & Morgan, G.B. (2017): Experimental crystallization of the Macusani Obsidian, with applications to lithium-rich granitic pegmatites. *J. Petrol.*, **58**, 1005–1030. https://doi.org/10.1093/petrology/egx044.
Ma, C., Beckett, J.R., Rossman, G.R. (2014): Monipite, MoNiP, a new phosphide mineral in a Ca-Al-rich inclusion from the Allende meteorite. *Am. Mineral.*, **99**, 198–205.
Matsubara, S., Miyawaki, R., Kurosawa, M., Suzuki, Y. (2003): Watatsumiite, $KNa_2LiMn_2V_2Si_8O_{24}$, a new mineral from the Tanohata mine, Iwate Prefecture, Japan. *J. Mineral. Petrol. Sci.*, **98**, 142–150.
Mills, S.J., Hatert, F., Nickel, E.H., Ferraris, G. (2009): The standardization of mineral group hierarchies: application to recent nomenclature proposals. *Eur. J. Mineral.*, **21**, 1073–1080.
Palme, H., Lodders, K., Jones, A. (2014): Solar system abundances of the elements. *in* "Volume 2: planets, asteroids, comets and the solar system", A.M. Davis, ed., Treatise on geochemistry (second edition), H. Holland, K. Turekian, eds. Elsevier, Oxford, 15–36.
Pekov, I.V. (1998): Minerals first discovered on the territory of the Former Soviet Union. Ocean Pictures, Moscow, Russia.
— (2000): Lovozero Massif: history, pegmatites, minerals. Ocean Pictures, Moscow, Russia.
Piantadosi, S.T. (2014): Zipf's word frequency law in natural language: a critical review and future directions. *Psychon. Bull. Rev.*, **21**, 1112–1130.
Pimm, S.L. & Jenkins, C.N. (2019): Connecting habitats to prevent species extinctions. *Am. Sci.*, **107**, 162–169.
Ramik, R.A., Sturman, B.D., Dunn, P.J., Povarennykh, A.S. (1980): Tancoite, a new lithium sodium aluminum phosphate from the Tanco pegmatite, Bernic Lake, Manitoba. *Can. Mineral.*, **18**, 185–190.
Rao, C., Hatert, F., Dal Bo, F., Wang, R., Gu, X., Baijot, M. (2017): Mengxianminite $(Ca_2Sn_2Mg_3Al_8[(BO_3)(BeO_4)O_6]_2)$ a new borate mineral from Xianghualing skarn, Hunan Province, China, with a highly unusual chemical combination (B + Be + Sn). *Am. Mineral.*, **102**, 2136–2141.
Rudnick, R.L. & Gao, S. (2014): Composition of the continental crust. *in* "Volume 4: the crust", R.L. Rudnick, ed., Treatise on geochemistry (second edition), H. Holland, K. Turekian, eds, Elsevier, 1–51.
Sabougni, M.L., Lin, P.L., Cerisier, P., Pelton, A.D. (1980): Computer analysis of phase diagrams and thermodynamic properties of cryolite based systems: I. The $AlF_3$-LiF-NaF system. *Metall. Trans. B*, **11**, 493–501.
Selway, J.B., Černý, P., Hawthorne, F.C., Novák, M. (2000): The Tanco pegmatite at Bernic Lake, Manitoba. XIV. Internal tourmaline. *Can. Mineral.*, **38**, 877–891.

Sharygin, V.V. & Vladykin, N.V. (2014): Mineralogy of cryolite rocks from the Katugin massif, Transbaikalia, Russia. *in* "Abstract Book of 30th International Conference on "Ore Potential of Alkaline, Kimberlite and Carbonatite Magmatism," 29 September – 02 October 2014 Antalya, Turkey", 166–168.

Stanley, C.J., Jones, G.C., Rumsey, M.S., Blake, C., Roberts, A.C., Stirling, J.A.R., Carpenter, G.J.C., Whitfield, P.S., Grice, J.D., LePage, Y. (2007): Jadarite, $LiNaSiB_3O_7(OH)$, a new mineral species from the Jadar Basin, Serbia. *Eur. J. Mineral.*, **19**, 575–580.

Stinton, D.P. & Brown, J.J. Jr. (1975): Phase equilibria in the system $Na_3A1F_6$-$Li_3A1F_6$. *J. Am. Ceram. Soc.*, **58**, 257.

—, — (1976): Phase equilibria in the system LiF-$AlF_3$-$Na_3AlF_6$. J. Am. Ceram. Soc., **59**, 264–265.

Torres-Treviño, G. & West, A.R. (1986): Compound formation, crystal chemistry, and phase equilibria in the system $Li_3PO_4$-$Zn_3(PO_4)_2$. *J. Solid State Chem.*, **61**, 56–66.

Van Velthuizen, J. & Chao, G.Y. (1989): Griceite, LiF, a new mineral species from Mont Saint-Hilaire, Quebec. *Can. Mineral.*, **27**, 125–127.

Wenger, M. & Armbruster, T. (1991): Crystal chemistry of lithium: oxygen coordination and bonding. *Eur. J. Mineral.*, **3**, 387–399.

Williams, H., Hoffman, P.F., Lewry, J.F., Monger, J.W.H., Rivers, T. (1991): Anatomy of North America: thematic geologic portrayals of the continent. *Tectonophysics*, **187**, 117–134.

Yang, Z., Giester, G., Ding, K., Tillmanns, E. (2011): Crystal structure of nanlingite – the first mineral with a $[Fe(AsO_3)_6]$ configuration. *Eur. J. Mineral.*, **23**, 63–71.

Zhabin, A.G. (1979): Is there evolution of mineral speciation on Earth? *Doklady Akad. Nauk*, **247**, 199–202. (in Russian; translation: Doklady Earth Science Sections, 247, 142–144).

Zhou, J. & Ning, D. (2017): Stochastic community assembly: does it matter in microbial ecology? *Microbiol. Mol. Biol. Rev.*, **81**, e00002–17, 1–32. https://doi.org/10.1128/MMBR.00002-17.

*Received 29 January 2019*
*Modified version received 26 April 2019*
*Accepted 30 April 2019*